Detailed Modeling of the Reaction of C 2 H 5 + O 2

ARTICLE *in* THE JOURNAL OF PHYSICAL CHEMISTRY A · APRIL 2005

Impact Factor: 2.69 · DOI: 10.1021/jp0451142 · Source: PubMed

3 AUTHORS, INCLUDING:

Chitralkumar V Naik
ANSYS
59 PUBLICATIONS **497** CITATIONS
SEE PROFILE

Anthony M Dean
Colorado School of Mines
158 PUBLICATIONS **3,949** CITATIONS
SEE PROFILE

Detailed Modeling of the Reaction of $C_2H_5 + O_2$

Hans-Heinrich Carstensen, Chitralkumar V. Naik, and Anthony M. Dean*

Chemical Engineering Department, Colorado School of Mines, Golden, Colorado 80401

Received: October 26, 2004; In Final Form: January 13, 2005

Modeling of low-temperature ethane oxidation requires an accurate description of the reaction of $C_2H_5 + O_2$, because its multiple reaction channels either accelerate the oxidation process via chain branching, or inhibit it by forming stable, less reactive products. We have used a steady-state chemical-activation analysis to generate pressure and temperature dependent rate coefficients for the various channels of this system. Input parameters for this analysis were obtained from ab initio calculations at the CBS-QB3 level of theory with bond-additivity corrections, followed by transition state theory calculations with Wigner tunneling corrections. The chemical-activation analysis used QRRK theory to determine $k(E)$ and the modified strong collision (MSC) model to account for collisional deactivation. This procedure resulted in a $C_2H_5 + O_2$ submechanism which was either used directly (possibly augmented with a few C_2H_5 generating and consuming reactions) or as part of a larger extended mechanism to predict the temperature and pressure dependencies of the overall loss of ethyl and of the yields of ethylene, ethylene oxide, HO_2, and OH. A comparison of the predictions using both mechanisms allowed an assessment of the sensitivity of the experimental data to secondary reactions. Except for the time dependent OH profiles, the predictions using the extended mechanism were in good agreement with the observations. By replacing the MSC model with master equation approaches, both steady-state and time dependent, it was confirmed that the MSC assumption is adequate for the analysis of the $C_2H_5 + O_2$ reaction. The good overall performance of the $C_2H_5 + O_2$ submechanism developed in this study suggests that it provides a good building block for an ethane oxidation mechanism.

Introduction

Reactions of alkyl radicals with molecular oxygen are very important in low-temperature oxidation (<1000 K) and atmospheric chemistry. This is due to the relatively long lifetime of both alkyl radicals and alkylperoxy intermediates under these conditions. The initially formed alkylperoxy radical is chemically activated and the subsequent reactions of this energized species involve the competition between unimolecular reactions and collisional stabilization. The stabilized adduct can subsequently react, with product channels identical to those of the energized adduct. Reactions of $RO_2^\bullet$ play a central role in low-temperature hydrocarbon ignition kinetics. This is exemplified by the kinetic mechanism discussed by Walker and Morley:[1]

$$R^\bullet + O_2 \rightleftharpoons RO_2^\bullet \quad (1)$$

$$RO_2^\bullet + RH \rightleftharpoons ROOH + R^\bullet \quad (2)$$

$$ROOH \rightleftharpoons RO^\bullet + OH \quad (3)$$

$$RO_2^\bullet \rightleftharpoons R^\bullet OOH \quad (4)$$

$$R^\bullet OOH \rightleftharpoons cyRO + OH \quad (5)$$

$$R^\bullet OOH + O_2 \rightarrow \text{chain branching} \quad (6)$$

Here $R^\bullet$ is an alkyl radical, cyRO is a cyclic ether, $RO^\bullet$ is an alkoxy radical, and $R^\bullet OOH$ is an alkylhydroperoxy radical. It is believed that the reversibility of (1) is responsible for the "negative temperature coefficient" (NTC) observed in alkane ignition between about 600 and 800 K. An important step in this mechanism is the isomerization of the alkylperoxy radical $RO_2^\bullet$ to form the alkylhydroperoxy radical $R^\bullet OOH$, because this leads to chain branching via (6).

Recent electronic structure calculations by Schaefer's group[2,3] on the $C_2H_5 + O_2$ system suggest that this mechanism is incomplete. On the basis of a proposal by Baldwin,[4] these researchers identified a new reaction channel for ethylperoxy, the *concerted* formation of HO_2 and C_2H_4:

$$CH_3CH_2OO^\bullet \rightleftharpoons C_2H_4 + HO_2 \quad (4a')$$

Prior to the identification of this pathway the formation of HO_2 and C_2H_4 was thought to proceed entirely sequentially via isomerization (to hydroperoxyethyl) followed by β-scission. The concerted HO_2 elimination should be possible for larger alkylperoxy systems as well, so that the Walker and Morley scheme needs to be expanded by (4a):

$$RO_2^\bullet \rightleftharpoons \text{olefin} + HO_2 \quad (4a)$$

The barrier for (4a′) was found to be several kcal/mol lower than that of the competing isomerization channel:

$$CH_3CH_2OO^\bullet \rightleftharpoons C^\bullet H_2CH_2OOH \quad (4')$$

Because the preexponential factors for both reactions are comparable (on the order of 10^{12} s^{-1}), the concerted elimination pathway dominates. As a result, chain branching via (6) should be less important than originally thought, and one expects that the overall ignition kinetics will be considerably slower. The inhibition of ignition due to the concerted elimination pathway should be most apparent for ethane because the isomerization

* Corresponding author. E-mail: amdean@mines.edu.

10.1021/jp0451142 CCC: $30.25
Published on Web 02/17/2005

can only occur via four- and five-member transition states with high barriers. For larger hydrocarbons, not only should the barrier for the five-member transition state be lower (if abstraction occurs from a CH_2 or CH moiety and not from a CH_3 group) but in addition isomerizations via six- or seven-member transition states are possible. These isomerizations likely have lower barriers than the concerted elimination, but most of them presumably also have lower *A*-factors, because additional rotors are tied up in the transition state. Thus the concerted elimination pathway might also affect the low-temperature hydrocarbon ignition kinetics of larger systems.

In this context there is a need to revisit low-temperature hydrocarbon ignition kinetics, with particular attention to the impact of the concerted elimination channel. Because ethane oxidation is the simplest system that involves this reaction, an analysis of $C_2H_5 + O_2$ is a logical starting point. Indeed, several theoretical treatments of this reaction, with a focus on the concerted elimination channel, have been published recently. Sheng et al.[5] used quantum Rice−Ramsperger−Kassel (QRRK) theory to calculate $k(E)$ and both a steady-state modified strong collision (MSC) and a master equation (ME) analysis to describe collisional deactivation. They successfully predicted ethylene and HO_2 yields as a function of pressure and temperature. Miller and co-workers[6−9] solved the time dependent master equation for $C_2H_5 + O_2$ and were able to describe the temperature dependence of the overall rate constant for ethyl consumption, the pressure dependence of the ethylene yield at 298 K, and the temperature and time dependence of the HO_2 and OH production. They also extracted time independent rate constants[9] (for $P = 0.039$, 1, and 10 atm) from their time dependent solutions to the master equation. However, despite these successes, neither of the available kinetic models is able to quantitatively predict all the experimental observations. For example, both models systematically underpredict the rate of ethyl consumption in the falloff regime at 298 K. Thus a direct incorporation of either of these mechanisms in an ethane oxidation model would compromise its validity. This current study is directed at producing apparent rate constants for the $C_2H_5 + O_2$ reaction that are more successful in describing the multitude of data reported for this system. Given the importance of the $C_2H_5 + O_2$ reaction for ethane ignition, we think such additional effort is warranted.

The reaction of C_2H_5 with O_2 has been subject of extensive experimental studies. Slagle et al.[10] investigated the temperature dependence of the overall rate constant for loss of C_2H_5 at several total gas densities. They also provided limited results for the ethylene channel. Plumb et al.[11] and Kaiser et al.[12] measured the pressure dependence of the overall rate constant at room temperature, and McAdam et al.,[13] Wallington et al.,[14] Wagner et al.,[15] and Kaiser et al.[16−18] provided temperature and pressure dependent ethylene yields. In addition, Baldwin et al.[19] and Kaiser[20] investigated the ethylene oxide product channel as a function of temperature. Finally, Clifford et al.[21] reported time profiles and temperature dependent yields of HO_2, and DeSain et al.[9] obtained time-resolved absolute OH data.

The wealth of available experimental data should provide a stringent test of specific features of the potential energy surface (PES). For example, the overall rate of ethyl loss is very sensitive to the $CH_3CH_2OO^{\bullet}$ well depth and to the properties of the variational transition state for the redissociation reaction. If, as the current consensus suggests, virtually all of the ethylene and HO_2 is produced via the concerted elimination channel, then the temperature and pressure dependence of their production rate is sensitive to the barrier height of this channel. Ethylene oxide can only be produced from the $C^{\bullet}H_2CH_2OOH$ isomer. Therefore, ethylene oxide rate data are expected to provide important information about this isomerization barrier.

Our analysis started with a high-level ab initio calculation of the underlying PES for the $C_2H_5 + O_2$ reaction. The results were used to calculate input parameters for the chemical activation analysis, such as thermodynamic properties of all species and high-pressure rate constants for the reaction channels. Pressure and temperature dependent apparent rate constants were obtained mainly from a QRRK/modified strong collision (MSC) analysis. In some instances we performed additional QRRK/steady-state master equation calculations to validate the results. The resulting sets of rate constants were incorporated into an extended mechanism and used to predict a wide range of experimental data taken from the literature, including the "final" products observed in end product studies of the $C_2H_5 + O_2$ system. We will show that these predictions are generally in good agreement with the data, but that some data are rather sensitive to secondary reactions. In the discussion section we analyze the importance of small but subtle changes, such as minor shifts of barrier heights and the effect of tunneling corrections on predicted ethylene yields. This section also provides a justification for the use of a larger than usual collision cross section, and it addresses the accuracy of time independent rate constants for this reaction system. Finally, we conclude by identifying some of the gaps in our understanding and suggest avenues of future research.

Calculation Methods

The potential energy surface was calculated using the CBS-QB3 compound method[22] as implemented in the Gaussian 98W software package.[23] This method provides geometries and frequencies at the B3LYP/6-311G(2d,d,p) level of theory. The frequencies were scaled by 0.99 prior to using them in the calculation of thermodynamic data, and vibrational modes resembling internal rotations were replaced by hindered rotors. We identified such modes, as well as the transition state structures, using the visualization software Molden.[24] The hindrance potentials for internal rotations were obtained as a function of the dihedral angle from relaxed surface scans at the B3LYP/6-31G(d,p) level of theory. These were then approximated with a Fourier expansion. The reduced moments of inertia for the internal rotations were calculated at the $I^{(2,3)}$ level as defined by East and Radom,[25] on the basis of the original work by Kilpatrick and Pitzer.[26] With this information at hand we can formulate and numerically solve the Schroedinger equation for each individual internal rotor, using the eigenfunctions of the 1-dimensional free rotor as basis functions. The energy eigenvalues are then used to calculate the contributions of each mode to thermodynamic properties via standard statistical mechanics methods.

The CBS-QB3 energies were used as originally defined, i.e., with the standard correction for spin contaminations. Recently, the magnitude of this correction has been questioned,[27,28] and a few examples seem to indicate that omission of this correction term leads to improved energies. Because these new findings have not yet led to an established revised procedure, we used the original CBS-QB3 method and note that a change of the spin contamination correction procedure would lead to only moderate changes of the PES.

The electronic energies were converted to heats of formation with the atomization method. This procedure was further improved by applying bond additivity corrections (BAC) as described by Petersson et al.[29] The BAC parameters were

TABLE 1: Lennard-Jones (LJ) Parameters Used To Calculate Apparent Rate Coefficients

species	collision diameter (σ_{LJ}) (Å)	well depths (ϵ_{LJ}) (K)
adduct $C_2H_5O_2$	4.94[a]	467.3
He	2.60	10.2
O_2	3.62	97.5
N_2	3.37	131.5

[a] The collision cross section was increased by a factor of 2.4 to fit falloff data as seen in Figure 2 (cf. text). This increase in collision cross section can also be achieved by increasing this collision diameter to approximately 8.24 Å (with He as a collider), 8.77 Å (with O_2 as a collider), or 8.63 Å (with N_2 as a collider).

obtained from a series of CBS-QB3 calculations for C/H/O containing molecules with well-established experimental heats of formation.

Canonical transition state theory (TST) was used to calculate high-pressure rate constants for all reaction channels with pronounced barriers. We used Wigner's method[30] to approximately account for contributions from tunneling to the rate constants. The high-pressure rate constant for the barrierless recombination of C_2H_5 with O_2 was not calculated in this work but taken from a variational TST analysis by Miller et al.[6]

Chemically activated reaction channels of the reaction of C_2H_5 with O_2 were then analyzed using a method described previously.[31] In short, QRRK theory was used to calculate energy dependent rate constants $k(E)$ and the modified strong collision (MSC) approach was employed to describe collisional deactivation. In some cases we replaced the MSC treatment with the steady-state master equation (ME) model described by Sheng et al.[5] Both calculations use, except for the energy transfer part, the same input parameters, which are the high-pressure rate constants discussed earlier, three-frequency representations[32] of the internal modes of the adducts, and estimated Lennard-Jones collision diameters (σ_{LJ}) and well depths (ϵ_{LJ}). These estimated Lennard-Jones parameters for the adduct $C_2H_5O_2$ and other bath gases are given in Table 1. The deactivation rate coefficient was computed as described earlier.[31]

The MSC model requires the average energy transferred per collision, $\langle E_{all} \rangle$ to calculate stabilization rate constants. In the ME code, the average energy transferred per down collision, $\langle E_{down} \rangle$, is used instead. We used a $\langle E_{down} \rangle$ value of 290 cm^{-1} for oxygen and nitrogen and 190 cm^{-1} for helium. The corresponding values for $\langle E_{all} \rangle$ were -154 cm^{-1} for oxygen and nitrogen, and -87 cm^{-1} for helium. These same values were used by Sheng et al.[5]

The pressure and temperature dependent rate coefficients obtained from the kinetic analysis were either fitted to a modified Arrhenius form for a specific pressure, or they were approximated with Chebyshev polynomials[33,34] over wide ranges of temperatures and pressures. The CHEMKIN 3.6.2 package[35] was used for the numerical integrations.

Results

Potential Energy Surface. The potential energy surface for the $C_2H_5 + O_2$ reaction, calculated at the CBS-QB3 level of theory, is shown in Figure 1. The major features of this surface are very similar to those calculated in earlier studies.[2,3,5−7] For example, the barrier for the concerted elimination is below the energy of the reactants whereas the barrier for isomerization is above it. Also, the barrier of the $CH_3CHO + OH$ channel is clearly higher than that for the H shift to form the $C^{\bullet}H_2CH_2OOH$ isomer. Not included in Figure 1 is the direct abstraction path. Previous studies concluded that this channel is not important for temperatures below 1000 K.

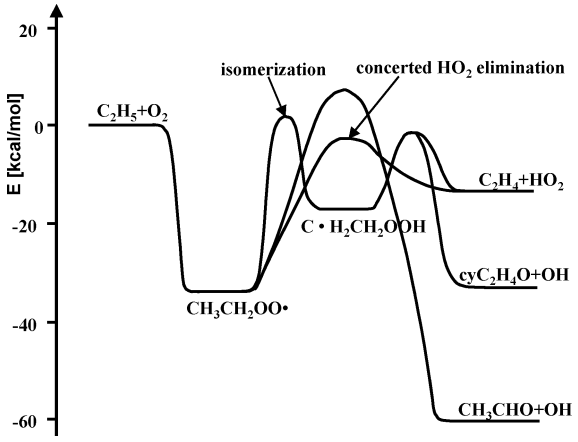

Figure 1. Potential energy surface for the reaction $C_2H_5 + O_2$ calculated at the CBS-QB3 level of theory at 0 K.

Because the overall features of the PES are well established, we will focus on some specific details of the CBS-QB3 results and compare those to other studies. We obtained for the C−O bond energy in $CH_3CH_2OO^{\bullet}$ a value of 34.0 kcal/mol at 0 K and 34.5 kcal/mol at 298 K. These values are in good agreement with the multistep calculations by Miller et al.[6] (33.9 kcal/mol at 0 K) and Sheng et al.[5] (35.3 kcal/mol at 298 K). They also agree reasonably well with the optimized well depth in Wagner et al.'s RRKM analysis[15] of this reaction (32.9 kcal/mol at 0 K and 34.1 kcal/mol at 298 K). In contrast, the calculations by Schaefer and co-workers[2,3] at the B3LYP and at the CCSD(T) levels yielded a weaker bond energy of ∼30 kcal/mol at 0 K. With respect to the barrier for the concerted elimination, our calculations located it 2.8 kcal/mol below the reactants at 0 K and 4.5 kcal/mol lower at 298 K. These results again compare well to 3.0 and 2.4 kcal/mol, reported by Miller et al. and Wagner et al., respectively, at 0 K and 4.8 kcal/mol reported by Sheng et al. at 298 K. As before, the results of Rienstra-Kiracofe et al.[3] deviate more, as they find the barrier to be only 0.9 kcal/mol (at 0 K) below the entrance channel. We found the barrier of the isomerization to β-hydroperoxyethyl to be 1.9 kcal/mol at 0 K and 0.8 kcal/mol at 298 K above the reactants. This is in reasonable agreement with the 3.1 kcal/mol (at 0 K) value reported by Miller et al. and the 1.0 kcal/mol (298 K) value of Sheng et al. Rienstra-Kiracofe et al. reported a substantially higher barrier of 5.3 kcal/mol (at 0 K) above the reactants for their highest level of theory. Finally, we compare the barriers for the two unimolecular product channels of β-hydroperoxyethyl with those from Miller et al. and Sheng et al. We found that the barrier for the channel to $C_2H_4 + HO_2$ is 1 kcal/mol (0 K) and 1.5 kcal/mol (298 K) below the reactants. Miller et al. determined this barrier to be 1.9 kcal/mol above the reactants at 0 K, whereas Sheng et al.'s result (1.5 kcal/mol below the reactants at 298 K) coincides with ours. We calculated the barrier for the $C_2H_4O + OH$ channel to be 1.0 kcal/mol below the reactants at 0 K and 1.7 kcal/mol below at 298 K. These results agree well with Miller et al. (0.6 kcal/mol below at 0 K) and Sheng et al. (2.1 kcal/mol below at 298 K). In summary, with exception of the barrier for $C^{\bullet}H_2CH_2OOH \rightarrow C_2H_4 + HO_2$, the results of this study agree well for all important stationary points of the PES with those of Miller et al. and Sheng et al., but they differ more from the calculations by Rienstra-Kiracofe et al.

Thermodynamic data for all species involved in the $C_2H_5 + O_2$ system are tabulated in Table 2. The complete set of thermodynamic data for all species of our extended mechanism is provided in the Supporting Information. The calculated heats

TABLE 2: Calculated Thermodynamic Data for Stable Species Involved in the Reaction $C_2H_5 + O_2$ [Heats of Formation in kcal/mol; Entropies and Heat Capacities in cal/(mol K)]

species	$\Delta_f H°_{298}$	$S°_{298}$	$C_p(300)$	$C_p(400)$	$C_p(500)$	$C_p(600)$	$C_p(800)$	$C_p(1000)$	$C_p(1500)$
C_2H_5	29.25	59.21	12.26	14.78	17.15	19.29	22.83	25.63	30.08
$CH_3CH_2OO^•$	−5.26	73.84	17.71	21.26	24.51	27.38	31.89	35.28	40.38
$C^•H_2CH_2OOH$	12.25	78.40	19.80	23.23	26.23	28.79	32.72	35.64	40.11
HO_2	3.13	54.68	8.29	8.84	9.39	9.89	10.68	11.28	12.26
OH	9.21	43.96	6.95	6.96	6.96	6.98	7.07	7.24	7.73
O_2	0.00	48.98	7.00	7.15	7.37	7.59	7.98	8.25	8.58
C_2H_4	12.46	52.33	10.19	12.55	14.76	16.69	19.83	22.25	26.06
CH_3CHO	−40.76	62.97	12.97	15.48	17.91	20.15	23.81	26.62	30.83
C_2H_4O	−12.74	57.99	11.38	14.83	17.91	20.54	24.53	27.43	31.69

TABLE 3: High-Pressure Rate Coefficients for the $C_2H_5 + O_2$ Reaction[a]

no.	reactions	A	n	E_a
1	$C_2H_5+O_2 \rightarrow CH_3CH_2OO^•$	2.91E+11	0.52	0.0
−1	$CH_3CH_2OO^• \rightarrow C_2H_5+O_2$	4.20E+15	0.0	34.1
2	$CH_3CH_2OO^• \rightarrow C^•H_2CH_2OOH$	1.92E+12	0.0	35.0
3	$CH_3CH_2OO^• \rightarrow CH_3CHO+OH$	1.23E+13	0.0	40.1
4	$CH_3CH_2OO^• \rightarrow C_2H_4+HO_2$	3.02E+12	0.0	30.5
−2	$C^•H_2CH_2OOH \rightarrow CH_3CH_2OO^•$	1.16E+11	0.0	17.2
5	$C^•H_2CH_2OOH \rightarrow C_2H_4+HO_2$	1.04E+13	0.0	16.4
6	$C^•H_2CH_2OOH \rightarrow C_2H_4O+OH$	7.84E+12	0.0	16.0

[a] The rate constant for (1) was taken from Miller et al.[6] and that for (−1) was calculated via microscopic reversibility. All other rate constants were computed with canonical transition state theory including Wigner tunneling corrections. Rate constants are given as $k = AT^n \exp(-E_a/RT)$, valid for 300−850 K. The units of A are s^{-1} (first order) and $cm^3\ mol^{-1}\ s^{-1}$ (second order), respectively, and E_a is given in units of kcal/mol.

of formation were corrected for systematic bond errors to improve accuracy. Though we shall not discuss all data in detail, some results are noteworthy. The heat of formation of ethylperoxy was calculated to be −5.3 kcal/mol, which is slightly higher (but within the error limits) than the experimental values reported by Knyazev et al.[36] (−6.5 ± 2.4 kcal/mol) and by Blanksby et al.[37] (−6.8 ± 2.3 kcal/mol). In case of C_2H_5, our heat of formation of 29.25 kcal/mol is 0.75 kcal/mol higher than the value recommended by Dobis et al.[38] With respect to entropy values, we see differences for C_2H_5, $C^•H_2CH_2OOH$, and C_2H_4O compared to Sheng et al.[5] In all three cases our calculations predict lower entropies (59.2 versus 60.6 cal/(mol K) for C_2H_5, 78.4 versus 81.9 cal/(mol K) for $C^•H_2CH_2OOH$, and 58.0 versus 59.4 cal/(mol K) for C_2H_4O). At this moment the cause for these differences is not clear. Additional details regarding the structure and energetics of all the species and transition states are available from the authors.

High-Pressure Rate Constants. Calculated high-pressure rate constants for the elementary reaction steps are presented in Table 3 for a temperature range of 300−850 K. In this range, simple Arrhenius expressions provide a good representation of the data. All rate constants were corrected for contributions from tunneling. We used Wigner's method[30] which only requires the imaginary frequencies (ν_{im}) of the transition states (scaled by a factor of 0.99) as input to calculate the transmission coefficient $\kappa(T) = 1 + (1/24)(1.44\nu_{im}/T)^2$. The effect of tunneling is higher for the isomerization reaction than the concerted elimination, with unscaled imaginary frequencies of −2273.2 and −1095.3 cm^{-1}, respectively. Table 3 also contains the high-pressure rate coefficient for the addition of C_2H_5 to O_2 which was taken from Miller et al.[6] The corresponding high-pressure rate constant for the redissociation of ethylperoxy back to the reactants was obtained using microscopic reversibility.

Inspection of the Arrhenius parameters for the key channels of the $C_2H_5 + O_2$ reaction system reveals two important facts: (1) The activation energy for the concerted elimination (rxn-4) is 4.5 kcal/mol lower than that for the isomerization of ethylperoxy (rxn-2), and it is 3.6 kcal/mol below the redissociation threshold (rxn-1). (2) The preexponential factor for the redissociation exceeds those of the concerted elimination and the isomerization by 3 orders of magnitude. From these observations it follows that the concerted elimination is the energetically preferred reaction channel of ethylperoxy. However, if sufficient thermal energy is available to break the C−O bond, the redissociation channel will dominate due to the higher preexponential factor. The relatively small preexponential factor and high activation energy make the isomerization path a minor product channel under all conditions.

$C_2H_5 + O_2$ Submechanism. The high-pressure rate coefficients given in Table 3 are the input parameters for the chemical and thermal activation analysis of the $C_2H_5 + O_2$ reaction. The results of this analysis at 1 atm total pressure and O_2 as bath gas are presented in Table 4 in modified Arrhenius form. We recognize three subsets of reactions: (1) the reactions of chemically activated ethylperoxy radicals, $C_2H_5O_2$*, which are directly formed when C_2H_5 and O_2 combine (rxn-1 to rxn-6); (2) the thermally activated unimolecular reactions of ethylperoxy (rxn-7 to rxn-11); (3) the thermally activated unimolecular reactions of hydroperoxyethyl (rxn-12 to rxn-15). These sets reflect a basic assumption in our analysis technique, which is that we can separate the overall reaction process into two steps: "direct" and "delayed." Initially, the chemistry is determined by reactions of the highly excited ethylperoxy radicals. These can react in one of two ways: either by forming bimolecular products or by stabilization via collisions. We refer to these reactions as "direct" channels because the products are a direct result of the $C_2H_5 + O_2$ association reaction. The "delayed" step occurs at sufficiently high temperatures where both stabilized adducts can undergo thermally activated unimolecular reactions on the time scale of some experiments. The "delayed" products from these reactions are formed in a sequential way (collisional stabilization followed by thermal dissociation).

According to Table 4, 15 apparent rate constants are required to describe the kinetics of the title reaction. It can be seen that our kinetic analysis produces for each reactant two apparent rate constants for the formation of $C_2H_4 + HO_2$. The reason for this is that these two channels are not identical. For $C_2H_5 + O_2$ or ethylperoxy as reactants, one of the rate constants describes the reaction proceeding via the concerted elimination path whereas the second one refers to the sequential path (isomerization followed by β-scission). For the case of hydroperoxyethyl as reactant, one path is the direct dissociation channel (via β-scission), and the sequential path is isomerization followed by concerted elimination. Thus, although the final products are the same, they are formed via two different mechanisms involving different transition states. The reactions of $C_2H_5 + O_2$ or ethylperoxy via the concerted elimination

TABLE 4: Apparent Rate Constants for the Reactions That Describe the $C_2H_5 + O_2$ System[a]

no.	reaction	A	n	E_a	k(600 K)	notes
1	$C_2H_5 + O_2 \rightleftharpoons CH_3CH_2OO^\bullet$	9.42E+36	−8.01	6.098	3.2E+12	
2	$C_2H_5 + O_2 \rightleftharpoons CH_3CHO + OH$	1.94E+12	−0.476	7.765	1.4E+08	
3	$C_2H_5 + O_2 \rightleftharpoons C_2H_4 + HO_2$	2.43E+17	−1.90	4.430	3.2E+10	concerted
4	$C_2H_5 + O_2 \rightleftharpoons C^\bullet H_2CH_2OOH$	8.84E+37	−9.33	10.159	2.1E+08	
5	$C_2H_5 + O_2 \rightleftharpoons C_2H_4 + HO_2$	1.02E+20	−2.97	8.639	4.2E+08	sequential
6	$C_2H_5 + O_2 \rightleftharpoons C_2H_4O + OH$	1.93E+20	−3.08	8.636	4.0E+08	
7	$CH_3CH_2OO^\bullet \rightleftharpoons CH_3CHO + OH$	2.13E+41	−9.81	45.919	2.3E−03	
8	$CH_3CH_2OO^\bullet \rightleftharpoons C_2H_4 + HO_2$	6.46E+30	−6.06	35.147	1.5E+01	concerted
9	$CH_3CH_2OO^\bullet \rightleftharpoons C^\bullet H_2CH_2OOH$	4.55E+51	−13.3	44.125	5.1E−02	
10	$CH_3CH_2OO^\bullet \rightleftharpoons C_2H_4 + HO_2$	4.47E+42	−10.1	44.734	2.6E−02	sequential
11	$CH_3CH_2OO^\bullet \rightleftharpoons C_2H_4O + OH$	3.01E+42	−10.0	44.609	2.7E−02	
12	$C^\bullet H_2CH_2OOH \rightleftharpoons CH_3CHO + OH$	3.10E+37	−10.1	28.588	1.3E−01	
13	$C^\bullet H_2CH_2OOH \rightleftharpoons C_2H_4 + HO_2$	5.65E+41	−10.9	26.490	6.1E+01	concerted
14	$C^\bullet H_2CH_2OOH \rightleftharpoons C_2H_4 + HO_2$	6.58E+41	−9.70	23.023	3.1E+06	β-scission
15	$C^\bullet H_2CH_2OOH \rightleftharpoons C_2H_4O + OH$	1.49E+41	−9.51	22.589	3.3E+06	

[a] The rate constants are valid for $P = 1$ atm, $T = 300-850$ K, and O_2 as collider. A factors are given in s^{-1} (first order) and $cm^3\ mol^{-1}\ s^{-1}$ (second order), and E_a is in given in kcal/mol.

channel are much faster than those via the sequential path. This can easily be seen from the rate constants at 600 K provided in Table 4. For example, the rate constant for rxn-3 (chemically activated concerted elimination channel) is about 76 times larger than that for rxn-5 (chemically activated sequential channel). Similarly, k(600 K) for rxn-8 (thermally activated concerted elimination channel) is about 580 times larger than that for rxn-10 (thermally activated sequential channel). In the case of the isomer hydroperoxyethyl, the $C_2H_4 + HO_2$ path via concerted elimination is a sequential reaction, because prior to the HO_2 elimination ethylperoxy must be formed via isomerization. Again we find that the multistep process is the slower one; rxn-13 is orders of magnitude lower than the β-scission channel (rxn-14) at 600 K.

The rate expressions in Table 4 are given in modified Arrhenius form that provides insight in the magnitude of the preexponential factor and the activation energy. However, for modeling purposes it is more convenient to use Chebyshev polynomials,[33,34] because this parametrization method is able to describe $k(T,P)$ data from multi-well reaction systems with good accuracy and relatively few parameters. Therefore the modeling results described later are done with rate constants in Chebyshev format. In the Supporting Information we provide such rate expressions for different colliders.

Extension of the Mechanism. The reactions listed in Table 4 are not sufficient to model $C_2H_5 + O_2$ experiments, because additional reactions describing the generation of C_2H_5 radicals or subsequent reactions of the products, especially HO_2 and $C_2H_5O_2$, are missing. Therefore we assembled a set of reactions based on a combination of literature review, theoretical calculations, and rate estimations that, combined with the subset given in Table 4, should largely account for the complete kinetics. However, the focus of this work is on the title reaction, and we consider the extended mechanism as preliminary and report it only as Supporting Information. Nevertheless, we will discuss important key reactions of it at the appropriate places in the main text. We designate the combination of the $C_2H_5 + O_2$ submechanism and these additional reactions as the expanded mechanism.

Predictions of Experimental $C_2H_5 + O_2$ Data. *A. Overall Rate Constant.* Measurements of the overall rate of the C_2H_5 loss as a function of He pressure at room temperature were performed in three laboratories. Plumb et al.,[11] Slagle et al.[10] and Wagner et al.[15] reported absolute rate constant measurements whereas Kaiser et al.[12] determined the rate constant relative to the reaction of $C_2H_5 + Cl_2$. Figure 2 contains plots

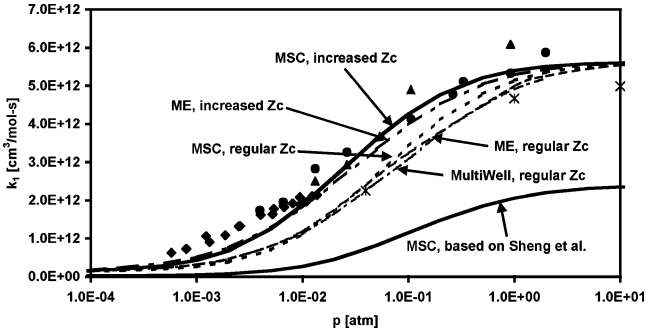

Figure 2. Comparison of the predicted (lines) and measured (filled symbols)[10−12] overall rate constants of the $C_2H_5 + O_2$ reaction vs pressure at 298 K using M = He. In addition, the total rate constants at three pressures reported by DeSain et al.[9] are shown (∗).

of some of these data together with several predictions as a function of pressure. The results from Kaiser et al. have been converted to absolute rate constants using a rate constant for $C_2H_5 + Cl_2$ of 6.5E+12•exp(+0.30 kcal/mol/RT) cm^3/(mol s). At 298 K, this expression yields the value reported by Timonen and Gutman[39] and is slightly smaller than the value used by Kaiser. When we first attempted to predict the experimental results using the Lennard-Jones collision parameters for ethylperoxy shown in Table 1, our predictions underestimated the loss rate of C_2H_5 in the lower pressure regime by a factor of approximately 2 (shown in Figure 2 as "MSC, regular Z_c"). The calculations were done in three different ways: (1) We extracted the rate constants directly from the chemical activation analysis. (2) We calculated C_2H_5 concentration versus time profile for conditions similar to those reported by Plumb et al. and Slagle et al. and extracted the total rate constant from the exponential decay. And (3) we performed the kinetic integration with the expanded mechanism and analyzed the final products as described by Kaiser[12] to obtain the rate constant relative to C_2H_5 with Cl_2. All three methods yielded almost the same values that are clearly lower than observed. To ascertain that this finding is not caused by a problem with our QRRK/MSC analysis, we repeated the analysis with a steady-state master equation code, still using QRRK theory to calculate $k(E)$ (shown in Figure 2 as "ME, regular Z_c"). The results confirmed the QRRK/MSC values and the inconsistency between experiments and predictions for lower pressures. In addition, we performed calculations with MultiWell, a stochastic code written and distributed by Barker.[40] $k(E)$ was calculated via inverse Laplace transformation of the same high-pressure rate constants that were used in the previous calculations. $\langle \Delta E_{down} \rangle$ was set at 200 cm^{-1},

and densities of states were calculated using the direct count method (by the Beyer−Swinehart algorithm). As shown in Figure 2, these predictions are in very good agreement with our master equation calculation and also fall well below the data. Finally, we used the rate coefficients provided by DeSain et al.[9] These rate constants were obtained from a RRKM/ME analysis using $\langle \Delta E_{down} \rangle = 200$ cm^{-1}. The results for 0.039, 1.0, and 10.0 atm are included in Figure 2, and it can be seen that they also underpredict the overall rate constant. In summary, independent of the sophistication of the analysis technique used, we consistently found clear deviations between the predictions and the well-established experimental data. This suggests that some of the input parameters are inappropriate. We tested the impact of the barrier heights for concerted elimination and isomerization, and we altered the well depth of $CH_3CH_2OO^{\bullet}$. No combination of changes within the estimated uncertainties of the PES calculations could resolve the differences. Finally we decided to increase the collision cross section to a value that provided a reasonable description of the data. We found that an increase of the collision cross section by a factor of 2.4 led to reasonable agreement except at the lowest pressures, as shown in Figure 2 by the curve labeled "MSC, increased Z_c". In addition we observed that the use of the steady-state ME method for collisional deactivation yields very similar results compared to the MSC approach (labeled "ME, increased Z_c" in Figure 2). All rate constants given in Table 4 have been calculated using the increased collision cross section.

Figure 2 also includes predictions based on the rate coefficients from Sheng et al.[5] These predictions are consistently lower than the data. The main reason for this discrepancy is that Sheng et al. used a different high-pressure rate constant for the $C_2H_5 + O_2$ recombination rate. Their value at 298 K is more than a factor of 2 lower than that used in this study. Interestingly, the high-pressure rate constant extracted from DeSain et al.[9] ($k \sim$ 5E12 cm^3/(mol s) at $P = 10$ atm) is also lower than the data and our predictions, although we used their high-pressure rate expression[6] in our analysis. Except for the possibility of uncertainties in the provided Arrhenius expressions, we do not have any explanation for this observation.

In Figure 2 we see that the experimentally obtained and the predicted rate constants seem to approach the high-pressure limit at approximately 1 atm. However, it appears as if the predictions are slightly below the observed data and one might be tempted to correct for this by adjusting the A factor of the rate constant for the recombination step. We preferred not to take this route, because the difference is only a few percent. The use of Miller et al.'s original high-pressure rate coefficients leads already to a substantial improvement of the prediction of the pressure dependence of the overall rate constant compared to earlier models. Recognizing that the small deviation observed can also easily be explained with uncertainties of the rate constant for the reference reaction, $C_2H_5 + Cl_2$, which was used to convert the relative measurements by Kaiser et al. to the absolute values shown in Figure 2, we believe that without additional experimental support a further adjustment is not warranted.

In the same spirit, we notice discrepancies (factor of up to ~2) between predicted and measured total rate constants at the lowest pressures. Given the simplified mechanism

$$C_2H_5 + O_2 \underset{k_{-1}}{\overset{k_1}{\rightleftharpoons}} [C_2H_5O_2]^* \xrightarrow{k_2} C_2H_4 + HO_2$$

$$\xrightarrow[+M]{k_3} C_2H_5O_2$$

we see that the formation of $C_2H_4 + HO_2$ from $[C_2H_5O_2]^*$ does not require collisions (although stabilization of the $[C_2H_5O_2]^*$ intermediate might increase the yield of $C_2H_4 + HO_2$ via thermally activated dissociation, compared to dissociation of $[C_2H_5O_2]^*$ back to $C_2H_5 + O_2$), whereas the yields of stabilized ethylperoxy will vanish for $[M] \rightarrow 0$. This explains the deviation of the falloff curve at low pressures from linearity. The fact that our model predictions underestimate the experimental data is this region suggests that the term $k_1 \cdot [k_2/(k_2 + k_{-1})]$ is too small. An increase of the high-pressure rate constant (k_1) would improve agreement with the experiments, but so would small changes in k_2 (which is related to the high-pressure rate constant for the concerted elimination reaction) and k_{-1}. Given this ambiguity, we did not attempt to adjust the underlying ab initio data.

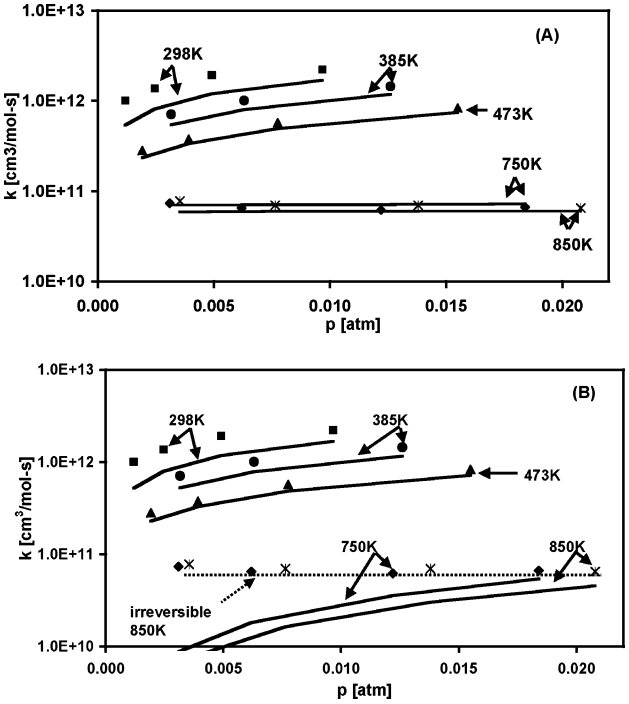

Figure 3. Comparison of the predicted and measured pressure dependence of the overall rate constant of the $C_2H_5 + O_2$ at different temperatures: (A) predictions with the expanded mechanism; (B) prediction with the $C_2H_5 + O_2$ submechanism. Full symbols represent the experimental data from Wagner et al.[15] (M = 80% He). Solid lines represent the predictions; the dashed line in (B) is obtained by making all bimolecular product channels irreversible.

Slagle et al.[10] provided additional pressure dependent data on the overall rate constant at higher temperatures ranging from 373 to 1002 K. The experiments were repeated in the same laboratory with an improved experimental setup a few years later,[15] and we only considered the newer data in this work. All measurements were done with helium as the major bath gas component (80%), which the remaining components being N_2 (at higher temperatures), O_2 and ethylbromide, which was used as precursor for ethyl radicals. Measurements were taken at 298 K, 385 K, 473 K, 640 K, 750 K and 850 K. In Figure 3A we compare these data sets to predictions with our expanded mechanism (adapted for He as collider). The first point to notice is that no results for 640 K are presented. Wagner et al. observed in their experiments that the C_2H_5 decay at this temperature displayed nonexponential behavior, and hence cannot accurately be described by a rate constant. Both of our modeling approaches were able to reproduce this nonexponential behavior. We will provide more discussion of this behavior later.

TABLE 5: Importance of the Stabilization and HO_2 Elimination Channels at 640 K as a Function of Reaction Time

	contribution to C_2H_5 depletion in %				
	1 ms	2.5 ms	5.0 ms	7.5 ms	10.0 ms
$C_2H_5O_2$ channel	41.4	38.7	34.2	29.8	25.8
$C_2H_4 + HO_2$ channels	57.2	59.7	64.1	68.4	72.3

Except for 298 K (Wagner et al.'s data were not included in Figure 2 but show the same factor of ~2 deviation as discussed earlier) the agreement between the expanded mechanism and the data is very good. (Additional calculations with O_2 as collider suggests that even better agreement can be reached if the collision properties of all gas components were accounted for.) More specifically, the predictions capture two important observations: (1) the negative temperature dependence of the total rate constant; (2) an increase of the pressure dependence with decreasing temperature. The negative temperature dependence is expected and caused by the increasing importance of the redissociation with temperature. This is the key reaction used to explain NTC behavior in the Walker−Morley scheme. The observed pressure dependence might be less obvious. At low temperatures collisional stabilization of chemically activated ethylperoxy radicals is the major reaction channel besides redissociation, and unless we are at the high-pressure limit, this channel introduces pressure dependency. With increasing temperature, bimolecular product channels become more and more important while the significance of the stabilization path decreases. Because these bimolecular product channels depend to a lesser degree on energy transfer processes, the overall pressure dependence declines and at 750 and 850 K no pressure dependence is either predicted or observed. This explanation suggests that Wagner's experimental data can solely be understood with the $C_2H_5 + O_2$ reaction system and consequently we should be able to reproduce the data with the reaction set given in Table 4. The results of such an attempt are shown in Figure 3B. At the lowest three temperatures we saw essentially no difference in both approaches. However, the simple reaction mechanism does not reproduce the pressure independent rate constants at 750 and 850 K. On the other hand, a rate analysis revealed that, besides the $C_2H_5 + O_2$ reactions, only the unimolecular decomposition of ethyl ($C_2H_5 \rightarrow C_2H_4 + H$) contributes significantly to the consumption of C_2H_5. Because this reaction does not depend on the O_2 concentration, it does not affect the apparent bimolecular rate constant. This apparent contradiction can be resolved by realizing that the basic mechanism does not allow the reaction products (mainly $C_2H_4 + HO_2$) to be consumed. The build-up of product concentrations leads to an increase of the reverse reactions forming $C_2H_5 + O_2$ and the apparent overall rate of consumption is reduced. By making the bimolecular product channels irreversible, as shown as broken line in Figure 3B for 850 K, the prediction of the short mechanism agrees well with the expanded mechanism and the data. The expanded mechanism contains fast secondary reactions of the bimolecular products (and of stabilized ethylperoxy) to make the $C_2H_5 + O_2$ product channels virtually irreversible. Thus the measured C_2H_5 decay data provide a good test case for the $C_2H_5 + O_2$ submechanism.

Finally we address the question why the C_2H_5 decay at 640 K occurs nonexponentially. To shed light on this problem, we performed a rate analysis for C_2H_5 at different reaction times. We found (Table 5) that the relative contributions of the stabilization and the HO_2 elimination channels to C_2H_5 consumption vary with reaction time. With increasing reaction time the stabilization of $C_2H_5O_2$ contributes effectively less and less

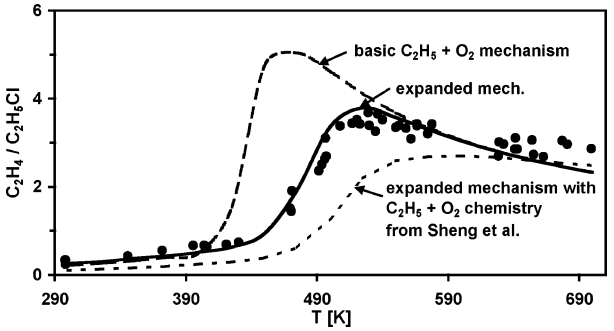

Figure 4. Comparison of predicted temperature dependences of ethylene production (lines), given as the ratios of ethylene to ethyl chloride, to the experimental results (symbols) reported by Kaiser.[20] See text for details.

to the overall decay because increasingly more stabilized $C_2H_5O_2$ is formed and produces C_2H_5 via thermal dissociation. At 640 K the time scales for the C_2H_5 decay and the thermal dissociation of ethylperoxy are comparable leading to the nonexponential time profile. At temperatures of 750 K and higher, thermal dissociation is much faster and a quasi equilibrium is established at early reaction times. Thus the observed rate constant is again exponential.

In summary, our model reproduces the overall rate constant for the reaction of ethyl with O_2 over a large temperature and pressure range reasonably well. To achieve this good agreement, we used in the kinetic analysis a collision cross section that is substantially larger than one would expect from commonly used estimations. Because an accurate reproduction of the overall rate constant is a prerequisite to accurately predict individual reaction channels, we kept this adjustment for all further calculations.

B. Ethylene Yields. Ethylene is a major product of the $C_2H_5 + O_2$ reaction at elevated temperatures and sufficiently low pressures. Its yield has been investigated by many investigators[11,15,17,18,20] at various conditions. In his most recent study, Kaiser[20] reported ethylene yields relative to ethyl chloride for a temperature range of 298−680 K. C_2H_5Cl is produced by the competing reaction of C_2H_5 with Cl_2. The isothermal experiments were carried out with mixtures of C_2H_6, O_2, and Cl_2 at a constant density of 6.74×10^{18} molecules/cm^3. Ethyl radicals were generated in the reaction of Cl atoms with ethane and Cl atoms in turn were produced via continuous UV photolysis of Cl_2. We used different mechanisms to predict these data. The shortest mechanism contained, besides the reaction set given in Table 4, only three additional reactions:

$$Cl_2 \rightarrow 2Cl \qquad \text{(rxn-1a)}$$

$$Cl + C_2H_6 \rightleftharpoons HCl + C_2H_5 \qquad \text{(rxn-2a)}$$

$$C_2H_5 + Cl_2 \rightleftharpoons C_2H_5Cl + Cl \qquad \text{(rxn-3a)}$$

The rate constant of the irreversible chlorine dissociation reaction was adjusted to reproduce the reported ethane consumption. We verified that the predictions are not very sensitive to moderate variations of this rate constant. For rxn-2a we used the same rate expressions as Kaiser; for rxn-3a we used the value discussed earlier, which is very similar to that used by Kaiser. As has been done in the experiments we extracted the C_2H_4:C_2H_5Cl ratios from extrapolations of the predicted species profiles to low ethane conversion.

An inspection of Figure 4 shows that this basic mechanism fails to predict the measured C_2H_4/C_2H_5Cl data in terms of the

location of the rapid increase as well as the quantitative values. On the other hand, good agreement between predictions and experiment was observed if we used our expanded mechanism for the calculations. This clearly indicates the importance of at least some secondary reactions. Similar to the findings for the total rate constant, the cause for these differences between both mechanisms is that the basic mechanism does not allow primary products, in this case stabilized ethylperoxy radicals, to react with other species in addition to thermal dissociation. This conclusion was verified by adding the following four reactions to the basic mechanism listed in Table 4:

$$HO_2 + HO_2 \rightarrow H_2O_2 + O_2 \qquad \text{(rxn-4a)}$$

$$C_2H_5O_2 + HO_2 \rightarrow C_2H_5OOH + O_2 \qquad \text{(rxn-5a)}$$

$$C_2H_5O_2 + C_2H_5O_2 \rightarrow C_2H_5O + C_2H_5O + O_2 \qquad \text{(rxn-6a)}$$

$$C_2H_5O_2 + C_2H_5O_2 \rightarrow C_2H_5OH + CH_3CHO + O_2 \qquad \text{(rxn-7a)}$$

With these additional reactions we got almost the same results as with the complete expanded mechanism, indicating the importance of these specific secondary reactions under these experimental conditions.

The effect of temperature on the C_2H_4:C_2H_5Cl ratio may be rationalized as follows: At low temperatures most of the chemically activated adduct is stabilized by collisions, but a small fraction yields $C_2H_4 + HO_2$. This "direct" product channel increases slowly with temperature. Between 450 and 500 K, a sharp increase of the C_2H_4:C_2H_5Cl ratio from ~1 to 3.5 is observed and this increase is captured by the model. The sudden increase is due to the onset of thermal dissociation of ethylperoxy, or, more precisely, due to the fact that its thermal dissociation becomes competitive to the consuming bimolecular reactions (recombination with itself or HO_2, rxn-5a to rxn-7a). Kaiser[20] also reasoned that the sharp increase was due to the opening of a new reaction channel. If the temperature is further increased, the ethylene yield starts to decline because the rate constant for redissociation of the stabilized adduct back to reactants increases. It can be seen that our model slightly overpredicts the peak value and the following decline of the C_2H_4:C_2H_5Cl ratio with temperature. As it turns out, the predicted ethylene yields are extremely sensitive to the barrier height of the concerted elimination channel and a minor change in the barrier height, within the uncertainties of the ab initio calculations, could improve our predictions. However, given the already good agreement and the uncertainties in the rate constant for $C_2H_5 + Cl_2$ and the secondary reactions, we chose to leave the input parameters unadjusted.

Figure 4 also contains predictions of an expanded mechanism that contained the $C_2H_5 + O_2$ subset reported by Sheng et al.[5] This group performed the kinetic analysis of the $C_2H_5 + O_2$ reaction prior to the date that the experimental data became available. Their model clearly captures the overall temperature dependence on the ethylene yield well, though its predictions are generally below the data. One reason for these deviations is the use of a lower high-pressure rate constant for the $C_2H_5 + O_2$ entrance channel in their analysis.

B1. Pressure Dependence of the C_2H_4 Yield at Room Temperature. Studies by Plumb et al.[11] and Wagner et al.[15] and the earlier work of Kaiser et al.[17,18] addressed the pressure dependence of the ethylene yield at room temperature. Plumb et al. and Wagner et al. determined ethylene yields relative to the initial ethyl concentrations using mass spectrometric detection. Kaiser et al. measured final ethylene and ethane concentrations with a gas chromatograph and calculated the ethylene yields from the ratio of ethylene over consumed ethane. We focus here on the results by Wagner et al. and Kaiser,[17] which combined cover a pressure range from nearly 0.001 atm to 1 atm with He or N_2/O_2/air as bath gas (Figure 5). As expected from the relative collision efficiencies, higher ethylene yields were observed in He. The yields decrease from about 24% at 0.0013 atm to 0.14% at 0.92 atm. The low-pressure results from Plumb et al. (not shown) are comparable to those from Wagner et al. with He as collider but show more scatter and are omitted for clarity.

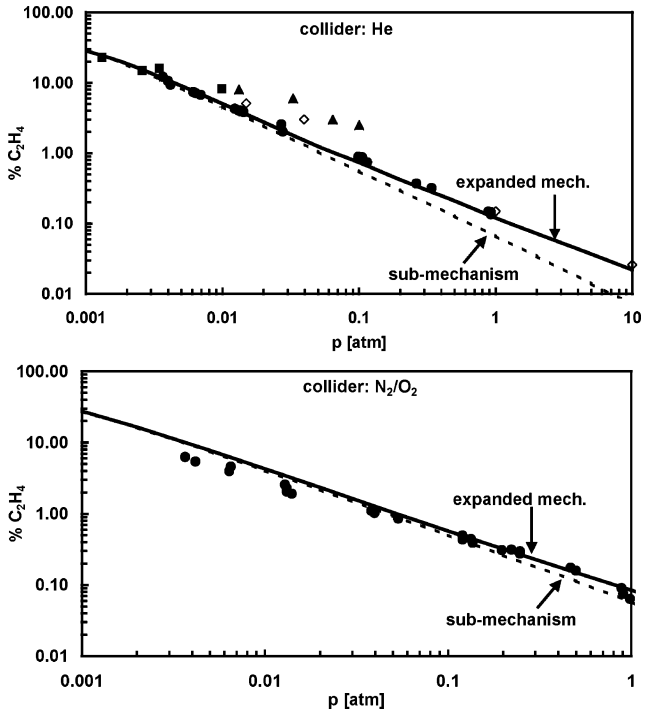

Figure 5. Comparison of the predicted and measured pressure dependence of the ethylene yield at 298 K. Filled symbols represent experimental data by Wagner[15] (squares), Kaiser[17] (circles), and Clifford[21] (triangles, inferred from HO_2 yields). Lines represent predictions with our mechanisms (cf. text), and the open diamonds are calculated with $C_2H_5 + O_2$ rate parameters from DeSain et al.[9]

As before, we performed calculations with either the basic mechanism given in Table 4 (complemented by the reactions rxn-1a to rxn-3a) or with the expanded mechanism. A comparison between both predictions then will reveal any sensitivity of the pressure dependent C_2H_4 yield measurements to secondary reactions. The top plot in Figure 5 contains the results for He as main collider. We notice that the predictions with the expanded mechanism agree very well with the experimental data whereas the use of the submechanism leads to clear deviations at higher pressure. This can be explained with the reaction

$$Cl + C_2H_5O_2 \rightarrow HCl + C_2H_4 + O_2 \qquad \text{(rxn-8a)}$$

in the expanded mechanism. We estimated the rate constant for rxn-8a by analogy to the H abstraction from ethane prior to modeling the ethylene yields. The lower part of Figure 5 contains the predictions for N_2 or O_2 as collider. In this case the predictions are less accurate, especially at low pressures, where the model predicts a higher ethylene yield than observed. Obviously, N_2 and O_2 are more effective colliders than assumed. Another difference between the He and N_2/O_2 cases is that the two mechanisms show less deviations. Although we did not analyze the cause in detail, it is possible that the higher collision

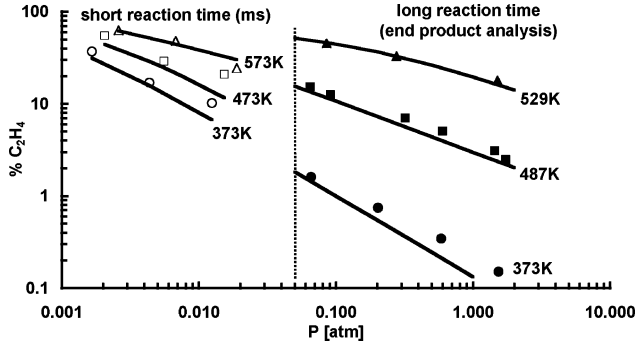

Figure 6. Comparison of the predicted and measured pressure dependence of the ethylene yield at several temperatures. Filled symbols represent the experimental data from Kaiser[18] using O_2 as collider, and open symbols represent the experimental data from Wagner et al.[15] (collider: He). Lines represent the predictions using the expanded mechanism.

efficiency leads to higher concentrations of $C_2H_5O_2$ radicals, which then probably recombine predominantly with themselves and with HO_2 radicals instead with Cl atoms. Figure 5 also includes predictions based on $C_2H_5 + O_2$ rate parameters from DeSain et al.[9] (open diamonds in the upper plot). The ethylene yields for He as collider calculated with their rate constants are consistently above our predictions (and especially at low pressures above the experimental data). Because we use a higher collision stabilization rate than DeSain et al., this difference is expected.

Ethylene and HO_2 are always produced together as coproducts, so that the HO_2 yield in the $C_2H_5 + O_2$ reaction should be identical to the ethylene yield. This allows us to include the experimental HO_2 yields from Clifford et al.[21] at 294 K and various pressures in Figure 5. At room temperature stabilized ethylperoxy does not dissociate thermally on the experimental time scale, and the "prompt" HO_2 yield is equal to the total HO_2 yield. Surprisingly, we find that the reported HO_2 yields are about a factor of 2−3 higher than the corresponding ethylene yields. In other words, the sets of ethylene and HO_2 data are inconsistent at room temperature, if the basic assumption is valid that the HO_2 yields originate exclusively from the $C_2H_5 + O_2$ reaction. We will come back to this issue when we take a closer look at the HO_2 measurements.

B2. Pressure Dependence of the C_2H_4 Yield at Elevated Temperature. Wagner et al.[15] and Kaiser[18] also measured the pressure dependence of the ethylene yield at temperatures above 298 K. In experiments with He as bath gas, Wagner et al. performed direct measurements of ethyl and ethylene time profiles up to 25 ms using a mass spectrometer. Ethylene yields are reported as the ratio of ethylene to the initial ethyl concentration. Kaiser, on the other hand, performed endproduct analysis experiments using a gas chromatograph. He measured the amounts of ethylene produced and ethane consumed at long reaction times (greater than 100 s) to calculate ethylene yields. The ethylene yields were corrected for the small amounts of C_2H_5 consumed in the reaction with Cl_2 using the measured amounts of C_2H_5Cl. Comparisons of predicted ethylene yields to both data sets are shown in Figure 6. (The absolute C_2H_4 yields at higher temperatures calculated for Kaiser's experimental conditions are sensitive to the assumed Cl_2 photolysis rate constant. Only the trends are meaningful.) The overall agreement is encouraging, because both the temperature and the pressure dependence of the ethylene yield is well captured. Furthermore, the two types of experiments performed by Wagner et al. and Kaiser et al. probe essentially two different aspects of the $C_2H_5 + O_2$ reaction. Due to the short reaction time and low pressures in Wagner et al.'s experiments, ethylene mainly originates from the "direct" chemically activated concerted elimination channel. On the other hand, Kaiser's endproduct results at relatively high pressures reflect the total ethylene yield ("direct" and "delayed") from both chemically and thermally activated channels. This also explains why the ethylene yields from Wagner et al. at 573 K are lower than those from Kaiser at 529 K. At these temperatures the delayed channels contribute significantly to the yields measured by Kaiser, but the unimolecular reaction rates are still too slow to be relevant under the conditions of Wagner et al.'s experiments.

In summary, we find overall good agreement between the experimental data shown in Figures 4−6 and predictions with our mechanism. This indicates that our model properly accounts for the temperature and pressure dependence of the ethylene production from both the "direct" and "delayed" channels. Although the experimental C_2H_4 yields are affected by secondary reactions (assuming that our expanded mechanism is reasonable), they nevertheless present a good test set for the $C_2H_5 + O_2$ reaction system.

C. Ethylene Oxide Yields. Ethylene oxide (C_2H_4O) has been measured as a minor product of the $C_2H_5 + O_2$ reaction at moderate temperatures and subatmospheric pressures.[19,20] In the most recent study Kaiser investigated the formation of ethylene oxide as a function of ethane consumption in the temperature range ∼500 to 650 K. The experimental conditions are the same as those for the temperature dependent ethylene yield study. Kaiser observed a linear relationship between the ethylene oxide concentration and the ethane consumption, and he used the slopes to determine temperature dependent ethylene oxide yields. In an earlier study, Baldwin et al.[19] used the thermal decomposition of tetramethylbutane (forming isobutyl radicals) in a C_2H_6/O_2 mixture to study the reaction products of $C_2H_5 + O_2$ as a function of temperature (673−813 K) at mainly 0.076 atm. Isobutyl radicals react with O_2 to produce HO_2 (+ isobutene) radicals, which either directly attack C_2H_6 to generate C_2H_5 radicals or they form OH radicals (via $2HO_2 \rightarrow H_2O_2 + O_2$ followed by $H_2O_2 \rightarrow 2OH$), which then abstract H atoms from ethane. Despite this rather complicated method to generate C_2H_5 radicals, the authors were able to obtain reproducible C_2H_4O:C_2H_4 product ratios via gas chromatographic detection. On average, the C_2H_4O:C_2H_4 ratio was found to be ∼1:100 with a tendency to increase with increasing temperature. Additional experiments at 0.66 atm did not reveal any obvious pressure dependence of this ratio, and results from separate experiments with H_2/O_2 mixtures as a radical source yielded very similar results compared to the tetramethylbutane/O_2 experiments.

The observations of Baldwin et al. that (1) C_2H_4 and C_2H_4O are the only two important product channels in their study and (2) the results are independent of pressure and composition (collider gas) allow us to convert their ratios to absolute ethylene oxide yields and to combine this data with that of Kaiser to expand the temperature range. As can be seen from Figure 7 agreement between both sets of data is not perfect: Kaiser reports an ethylene oxide yield approximately twice that of Baldwin.

We performed three sets of calculations to model the data. Besides the use of the basic and the expanded mechanism, we also employed a modified expanded mechanism in which we removed the reaction

$$C_2H_4 + HO_2\,(+M) \rightarrow C_2H_4O + OH\,(+M) \qquad \text{(rxn-9a)}$$

The idea behind removing rxn-9a is that HO_2 radicals might undergo fast secondary reactions in Baldwin et al.'s experiments,

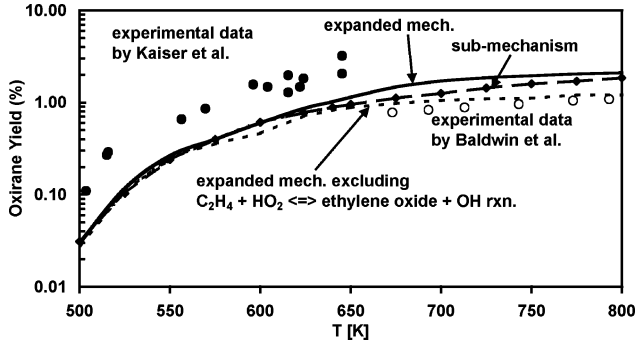

Figure 7. Comparison of experimentally observed[19,20] and predicted temperature dependent ethylene oxide yields at a total density of 6.8×10^{18} molecules/cm^3.

which would keep their concentration low and make contributions by rxn-9a unimportant. Because our extended mechanism does not contain species such as isobutene, we might overpredict the ethylene oxide yield with the expanded mechanism. All calculations are essentially done in analogy to Kaiser's experiments, and for most conditions they confirmed an approximately linear relationship between ethylene oxide yield and ethane consumption. However, the slopes were smaller than those seen by Kaiser, so that all calculations underpredicted his reported ethylene oxide yields. On the other hand, the predictions with all three mechanisms are above the data by Baldwin et al. Below about 625 K differences between the mechanisms are rather small indicating that the $C_2H_5 + O_2$ subset captures the formation of ethylene oxide. Above this temperature the expanded mechanism predicts the highest ethylene oxide yields due to significant contributions from rxn-9a. This can be seen from the predictions with the modified expanded mechanism. This mechanism leads to the lowest ethylene oxide yields, which agree well with the data by Baldwin et al.

At this point our mechanism appears to provide support for Baldwin et al.'s lower ethylene oxide yields. But, given the straightforward nature of Kaiser's experiment, one might also ask what changes of our expanded mechanism would be needed to better predict his data. Because the isomerization from ethylperoxy to hydroperoxyethyl is the limiting step in the formation of ethylene oxide, this barrier would have to be adjusted. We found that decreasing the barrier by 1.0 kcal/mol leads to a good reproduction of the measurements (but obviously would lead to larger discrepancies with Baldwin's data). This variation is within the expected uncertainty of the CBS-QB3 method.

In summary, the two experimental data sets bracket our predictions. Secondary reactions such as rxn-9a or the reaction sequence

$$Cl + C_2H_5OOH \rightarrow HCl + C^{\bullet}H_2CH_2OOH \qquad \text{(rxn-10a)}$$

$$C^{\bullet}H_2CH_2OOH \rightarrow C_2H_4O + OH \qquad \text{(rxn-11a)}$$

contribute to some extent to the ethylene oxide formation, which explains the "bumpy" temperature dependence. But the major source for ethylene oxide is the $C_2H_5 + O_2$ system and its yields, especially at lower temperatures, provide good test sets to validate our understanding of this reaction.

D. HO_2 Yields. HO_2 is the coproduct of C_2H_4 in the reaction of C_2H_5 with O_2, and complementary HO_2 measurements can be used to validate conclusions drawn from the ethylene data. However, experiments involving HO_2 are difficult to perform and to analyze; HO_2 is a reactive radical that easily undergoes

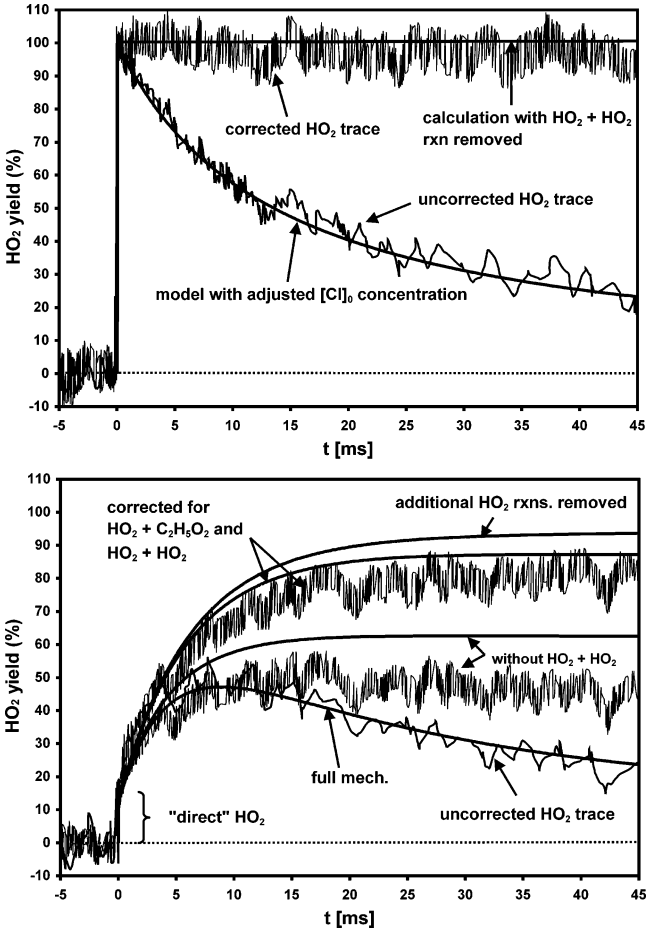

Figure 8. Modeling of the experimental HO_2 time profiles at $T = 648$ K and 0.066 atm (conditions: 85.9% He, 13.3% O_2, 0.67% CH_3OH or C_2H_6, and 0.13% Cl_2). Top: uncorrected and corrected profiles in the reference reaction. Bottom: uncorrected and corrected HO_2 profiles in the $C_2H_5 + O_2$ system. The HO_2 traces were scanned from Clifford et al.[21] (Figures 3 and 4). See text for details.

secondary reactions. Detection of HO_2 requires relatively high concentrations, which makes it impossible to suppress the $HO_2 + HO_2$ self-reaction. Because of the second-order character of the self-reaction and other side reactions, the evaluation of HO_2 experiments requires knowledge of its absolute concentration.

Clifford et al.[21] took on the difficult task of measuring HO_2 yields from the reaction $C_2H_5 + O_2$. In their experiments, C_2H_5 radicals were generated via the reaction of C_2H_6 with Cl atoms, which in turn were produced via pulsed laser photolysis of a suitable precursor. HO_2 was detected via multipass IR absorption. The reaction

$$C{\cdot}H_2OH + O_2 \rightleftharpoons CH_2O + HO_2 \qquad \text{(rxn-12a)}$$

was used to convert the measured absorption signals into absolute concentrations. Recognizing the importance of secondary reactions, Clifford et al. corrected their observed yields for consumptions via reactions rxn-4a and rxn-5a. This was demonstrated in detail for a particular measurement at 648 K, and we used this data set as starting point for our modeling. Figure 8 shows the results of our attempt to reproduce the methodology used by Clifford et al. to correct the HO_2 signal for secondary reactions. The initial chlorine concentration from the photolysis is unknown and has to be determined from the reference reaction by adjusting its value so that the observed time profile is reproduced. This profile essentially depends only on rxn-4a as the top plot of Figure 8 demonstrates. Once the

initial chlorine concentration is determined, we can use this value to model the $C_2H_5 + O_2$ reaction. As can be seen from the bottom plot of Figure 8, we achieved excellent agreement with the uncorrected experimental HO_2 profile. This is encouraging for at least two reasons: (1) Being able to reproduce the rising part of the HO_2 time profile, including the contribution of "direct" HO_2, confirms our treatment of the chemically activated $C_2H_5 + O_2$ reaction system at this temperature. (2) The agreement of the decay suggests that the extended mechanism is complete with respect to the important HO_2 consuming reactions. Because both the production and consumption rates are well reproduced, the absolute HO_2 yield is necessarily captured as well.

The additional profiles and plots in Figure 8 make clear how difficult it is to calculate the HO_2 yields in the $C_2H_5 + O_2$ reaction from the measurements. Clifford et al. used a rather complicated mathematical approach to account for the experimental contributions of reactions rxn-4a and rxn-5a. On the other hand, such corrections are much easier to achieve in the modeling study by simply removing the reactions in question from the mechanism. Surprisingly, we find significant differences in the corrected profiles although we used the same rate constants. In particular, our calculations suggest that the HO_2 recombination reaction reduces the HO_2 concentration significantly more than expected by Clifford et al. This difference is in part compensated by the second correction step, which deals with the impact of reaction rxn-5a. Nevertheless, we arrive at a slightly higher corrected HO_2 yield than Clifford et al., despite the good initial agreement with the observed profile. In addition, our rate analysis revealed that several other reactions such as

$$C_2H_5 + HO_2 \rightarrow C_2H_5O + OH \qquad \text{(rxn-13a)}$$

$$CH_3O_2 + HO_2 \rightarrow CH_3OOH + O_2 \qquad \text{(rxn-14a)}$$

play a role in HO_2 consumption, and, although these reactions yield OH radicals which will largely reproduce C_2H_5 radicals, we observed a clear increase of the HO_2 yield after removing these reactions from the mechanism (cf. the plot marked "additional HO_2 rxns removed" in Figure 8). As a result, our calculations predict approximately 10% higher corrected HO_2 yield than Clifford et al. for the 640 K experiment. To complete this discussion, we should mention that HO_2 production at longer reaction times is also impacted by reactions other than $C_2H_5 + O_2$. The most obvious one is the reaction

$$C_2H_5O + O_2 \rightarrow CH_3CHO + HO_2 \qquad \text{(rxn-15a)}$$

because ethoxy radicals are rapidly formed via ethylperoxy recombination. Given all these secondary reactions, it becomes clear that the HO_2 data have only a limited value as test case for the $C_2H_5 + O_2$ reaction per se, but they provide a good opportunity to validate the complete mechanism.

Having realized that our analysis leads to a slightly different interpretation of the raw data, one would expect small deviations over the entire temperature range covered in the study by Clifford et al. Figure 9 presents a comparison of the reported corrected total HO_2 yields with our predictions. Our MSC mechanism accurately captures the sharp increase in the HO_2 yield near 550 K. As seen previously for ethylene, it is the onset of thermal dissociation of ethylperoxy that is responsible for this behavior. Figure 9 also contains predictions with the steady-state QRRK/ME mechanism. Clearly, a change of the energy transfer model from MSC to ME has a minimal impact on the predicted total HO_2 yields.

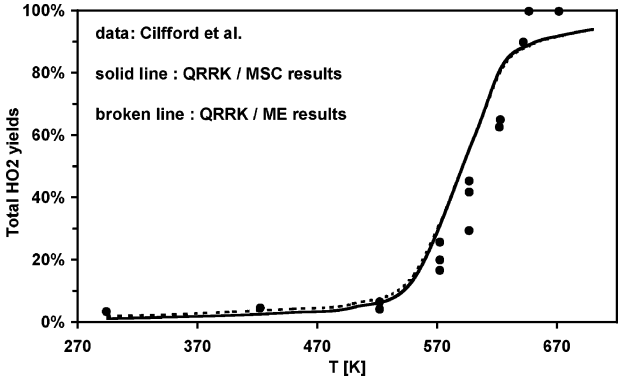

Figure 9. Comparison of the predicted temperature dependence of the "total" HO_2 yield to that measured by Clifford et al.[21] at a constant density of 1.1×10^{18} molecules/cm^3.

Both collision models yield room-temperature HO_2 yields that are clearly below the reported value. These differences are, however, consistent with the observations that the HO_2 yields by Clifford are about a factor of 2−3 higher than one would expect from complementary C_2H_4 yield data (cf. Figure 5). Because we could reproduce the ethylene data well, our model must differ from the corresponding HO_2 measurements. A second discrepancy is the exact location (temperature) at which the sharp increase in HO_2 occurs. Our model predicts this transition to happen at a slightly lower temperature than experimentally observed. Some of this difference might be attributed to the fact that our predicted HO_2 yields are expected to be slightly higher than those reported, as discussed above.

The rapid increase of the total HO_2 yield near 550 K is similar to the increase seen for the ethylene yield (Figure 4) at around 450 K. The shift in temperature for the onset of thermal dissociation of ethylperoxy can be explained by differences in the conditions for which the HO_2 and C_2H_4 experiments were performed: Clifford et al. conducted their experiments at a significantly lower pressure, $\sim^1/_6$th that of Kaiser. At any given temperature, lowering the pressure outside the high-pressure region has two effects: (1) it reduces the amount of stabilization, and (2) it reduces the rate constant for thermal dissociation of the stabilized adduct. The first effect influences the ratio between prompt and delayed HO_2 yields. If substantial amounts of ethylperoxy are produced, then the second effect determines how fast "delayed" HO_2 is formed and thus whether it contributes to the HO_2 signal detected at 17 ms reaction time. Therefore the amount of detectable "delayed" HO_2 produced via the thermal activation channel of ethylperoxy shows a shift toward higher temperature as the pressure is reduced. Not only did Kaiser use a higher total pressure in his experiments, but also the ethylene yields were measured at much longer reaction times. Therefore one expects that the thermally produced ethylene would contribute at much lower temperatures to the measured total ethylene yields. These arguments are augmented by our previously made observation that secondary reactions have an impact on the location of the sharp increase because thermal dissociation competes with bimolecular consumption reactions.

In conclusion, our model accurately predicts the total HO_2 yields over a wide temperature range. It also allows us to explain the temperature shift seen for the sharp increase of HO_2 yields compared to the C_2H_4 results by Kaiser. From the detailed analysis of measured HO_2 time profiles we conclude that the HO_2 measurements are significantly impacted by secondary reactions, which makes it difficult to use these data as stringent test set for the $C_2H_5 + O_2$ reaction itself. Difficulties in the

interpretation of the experiments might be the cause for the apparent inconsistency of the HO_2 and C_2H_4 yields at room temperature.

E. OH Time Profiles. OH is a coproduct with both ethylene oxide and acetaldehyde in the $C_2H_5 + O_2$ reaction, and OH profiles could in principle provide complementary information for these channels. In fact, because it is difficult to separate acetaldehyde formed in the $C_2H_5 + O_2$ reaction from that produced in subsequent reactions, the OH profiles might be the only data that can be used to characterize this channel. Due to its reactive nature, such measurements and their interpretation face challenges similar to those discussed for HO_2. DeSain et al.[9,41] have recorded OH time profiles over a time scale of 2 ms at low pressure and several temperatures between 296−700 K. The OH profiles were quantified by comparing them to signals from the reaction of HO_2 (from $C^{\bullet}H_2OH + O_2$, rxn-12a) with NO under similar conditions. To analyze the experimental data, DeSain et al. developed short reaction mechanisms for the reference and the $C_2H_5 + O_2$ systems. Their $C_2H_5 + O_2$ mechanism includes several reactions of the chlorine precursor ($CFCl_3$) and of the photolysis fragment $CFCl_2$, which emphasizes the sensitivity of the observed OH profiles to secondary reactions. Despite the introduction of these reactions, the authors are only able to qualitatively reproduce the OH time profile in the $C_2H_5 + O_2$ system.[9,41]

When we applied our expanded mechanism, augmented by the $CFCl_2$ and $CFCl_3$ reactions provided by DeSain et al., we observed that the model failed to predict the observed OH decay at longer times. We observed similar problems when we used the short reaction mechanism proposed by DeSain et al. In contrast to the observations, both calculations suggest a continued significant production of OH radicals at larger reaction times due to regeneration of C_2H_5 radicals (via rxn-16a) or the formation of CH_3 radicals (via the thermal dissociation of ethoxy radicals, rxn-17a).

$$OH + C_2H_6 \rightarrow H_2O + C_2H_5 \qquad \text{(rxn-16a)}$$

$$C_2H_5O \rightarrow CH_3 + CH_2O \qquad \text{(rxn-17a)}$$

Because the HO_2 concentrations are relatively high, the alkyl radicals as well as the photodissociation fragment $CFCl_2$ can react directly with HO_2 to yield OH.

$$R + HO_2 \rightarrow RO + OH \qquad R = CH_3, C_2H_5, CFCl_2 \qquad \text{(rxn-18a)}$$

Although we could identify this reaction sequence to be mainly responsible for the discrepancy between the observed OH profiles and our predictions, we were not able at this point to resolve this issue. Clearly, a more detailed mechanism needs to be developed, but this is beyond the scope of this study.

The fact that we are not able to predict the full time profile of the OH measurements by DeSain et al. leaves us with the question whether the experimental OH peak concentrations can be related to the OH yield from the $C_2H_5 + O_2$ reaction. Because the rise time of the OH signals is much faster than its decay, such a relation would be expected if the initial OH concentration is mainly produced via this reaction. We can address this problem by calculating the temperature dependent OH yield with our reaction set in Table 4 by making all bimolecular product channels irreversible. The ratio of final OH to initial C_2H_5 provides us with the OH yield. In Figure 10 we present a comparison of the experimental peak OH concentrations (normalized to the initial Cl atom concentration) to the OH yield expected from our kinetic analysis of the $C_2H_5 + O_2$ system.

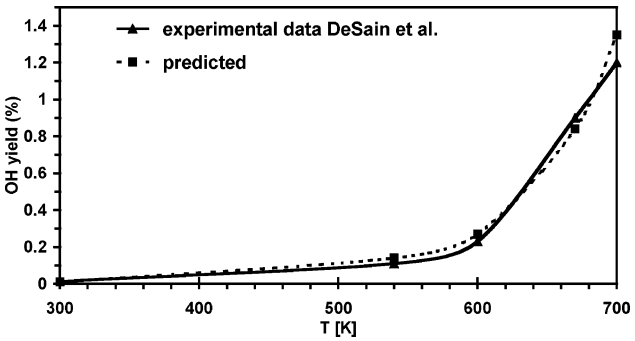

Figure 10. Comparison between predicted and measured[9] temperature dependent OH yields in the $C_2H_5 + O_2$ reaction at a total density of 3.25×10^{17} molecules/cm^3. See text for details.

The agreement is surprisingly good, suggesting that the measurements by DeSain et al. indeed captured the OH yield of $C_2H_5 + O_2$. However, more work is needed to clarify the kinetics at longer times.

In addition to predictions of the OH yields at different temperatures, our results also reveal which channels contribute to OH production. At 300 K the small OH fraction originates almost entirely from the ethylene oxide channel, but at 600 K about 15% of the OH is produced from the acetaldehyde channel. This fraction increases to about 25% at 700 K. The analysis makes clear that the aldehyde path, despite its higher barrier, becomes competitive to the isomerization channel as the temperature increases. For example, if we assume that the $[OH]_{peak}/[Cl]_0$ ratio of 1.2 reported by DeSain et al. for 700 K corresponds to the total OH yield in $C_2H_5 + O_2$, then we would expect an ethylene oxide yield of 0.9% at this temperature. The data by Baldwin et al.[19] suggest the ethylene oxide yield to be about 0.85%.

To summarize this discussion, the experimental OH data by DeSain et al. provide a very valuable but challenging data set. The interpretation of the measured peak concentrations as OH yields in the $C_2H_5 + O_2$ is consistent with our kinetic analysis of this system. In the temperature region of the NTC behavior OH is produced via two pathways (ethylene oxide or acetaldehyde) and the OH yield measured at 700 K fits well to the ethylene oxide yield reported by Baldwin et al. Despite this consistent picture, it is troubling that our full model is not able to reproduce the measured OH time profiles. Additional work to identify possibly missing reactions (including those of the precursor species $CFCl_3$) is needed, but this is outside of the scope of this work.

F. Final Products. In the previous sections we extensively used our $C_2H_5 + O_2$ submechanism in connection with an extended mechanism. The purpose was to probe whether the experimental data were mainly sensitive to the $C_2H_5 + O_2$ reaction or whether secondary reactions play a significant role. Although the extended mechanism is provided as Supporting Information, we did not discuss it in detail nor did we so far provide any validation of its performance. One way to test its validity is to apply it to predict the final products that are observed in end product studies[20,42,43] of the $C_2H_5 + O_2$ reaction. At room temperature the major products are acetaldehyde, ethylhydroperoxide, and ethanol, whereas at higher temperature other product such as ethylene, formaldehyde, CO and CO_2 are produced as well.

F1. Predictions of Room-Temperature Product Yields. Final products from the reaction of ethyl radicals with molecular oxygen have been reported by Niki et al.,[42] Wallington et al.,[43] and Kaiser.[20] Kaiser reports the product composition for the

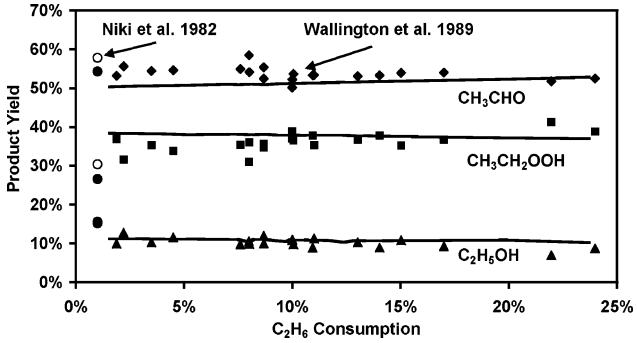

Figure 11. Modeling of the final products observed in the $C_2H_5 + O_2$ experiments by Wallington et al.[43] and Niki et al.[42] Symbols present normalized experimental data and lines show the results of the calculations.

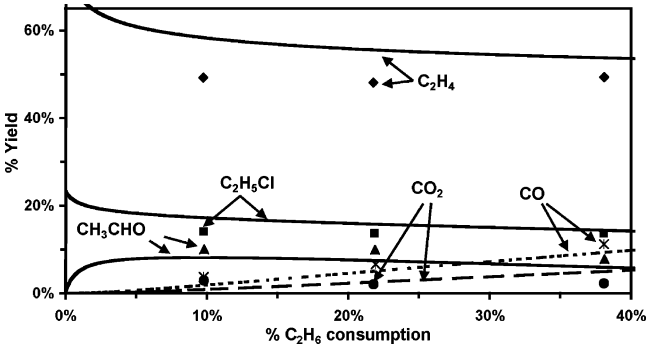

Figure 12. Modeling of the final product yields measured by Kaiser[20] at 577 K. Filled symbols represent the experimental data and lines represent predictions using the expanded mechanism. Kaiser also reports 15−20% formaldehyde and 2.4% methyl chloride.

C_2H_4 yield experiments that were discussed earlier (cf. Figure 4). He found about 63% acetaldehyde (obtained by extrapolating to zero ethane conversion), small yields of ethylene and ethyl chloride and nonquantified amounts of ethanol. The third major product expected in these experiments, ethylhydroperoxide, could not be identified. Acetaldehyde is not directly produced in the reaction of $C_2H_5 + O_2$ (the high barrier makes this channel at room temperature unimportant), but mainly in the recombination reaction of ethylperoxy radicals (rxn-7a). Ethylhydroperoxide will be produced similarly via the reaction of ethylperoxy with HO_2 (rxn-5a). A possible explanation for the missing ethylhydroperoxide is that it might have decomposed on the wall or in the GC. This problem and the consequently incomplete carbon mass balance make it difficult to use this most recent study for quantitative comparison. Instead we focus here on the earlier FTIR studies by Niki et al. and Wallington and co-workers. Niki et al.[42] observed all three major products in experiments of Cl initiated oxidation of ethane in O_2-N_2 mixtures at 0.92 atm and 298 K. Very similar experimental data are reported by Wallington et al.[43] at 295 K and 0.92 atm. Because Wallington et al. report detailed experimental conditions, we were able to apply our model to exactly the same conditions. The results are shown in Figure 11, in which we also included the results from Niki et al.'s study. To arrive at the plotted normalized yields, we assumed that the three products add up to 100% (the calculations suggest that these three products contribute to > 96% of the products). This procedure removed much of the scatter, which is largely caused by the low accuracy of the ethane consumption values. In the original work, Wallington reports an average acetaldehyde yield of 54 ± 14% and the large error margin reflects the uncertainties mentioned above. After the normalization procedure we find an acetaldehyde yield of 51.2%. Similarly the results for ethanol and ethylhydroperoxide differ slightly from the original work. An inspection of Figure 11 shows that our predictions (also normalized as described above) agree to within a few percent with Wallington's measurements. For example, the predicted average acetaldehyde yield is found to be 50.7%, and for ethylhydroperoxide we predict an average yield of 38.5% compared to 37.8% from experiment (originally reported: 36 ± 10%). Niki et al.'s data in general are consistent with Wallington's, although the absolute values differ by a few percent.

A possibly important discrepancy between measurement and prediction is in the dependence of the product yields on ethane consumption. The measured acetaldehyde yields appears to slightly decline with increasing ethane consumption, but the model predicts a small increase. The opposite is true for ethylhydroperoxide. The acetaldehyde yields in Kaiser's work support Wallington's measurements, hence confirming the problem. These observations could be used in the future to further improve the mechanism.

F2. Predictions of Product Yields at 577 K. Figure 12 shows selected product profiles of Kaiser's $C_2H_5 + O_2$ experiment at 577 K. The product spectrum at this temperature is drastically different for the room-temperature case. For example, ethylhydroperoxide is no longer stable, and hence the problems discussed for the 298 K experiments do not arise here. The higher temperature leads to two important changes: (1) the onset of the thermal dissociation of the stabilized adduct $CH_3CH_2OO^{\bullet}$ leads to higher ethylene yields as can be deduced from the high C_2H_4/C_2H_5Cl ratios seen in Figure 4, and (2) the overall rate constant is in the falloff region and consequently the reaction of C_2H_5 with Cl_2 becomes more competitive. This explains the high concentration of ethyl chloride. Agreement between our prediction and these two major products is reasonable but not perfect. More specifically, the model predicts an ethylene yield of 54−58% depending on the degree of ethane consumption. In contrast, the experimentally observed yield is around 49% and constant. For ethyl chloride we calculate at 10% ethane conversion a yield of ∼17.5% compared to 14% measured. Given these differences one might ask why we observed in Figure 4 such a good agreement between calculated and measured C_2H_4:C_2H_5Cl ratio. The reason is that these ratios were determined at low conversions (as done in the experiment) and because the model overestimates both yields in a similar way, the predicted and measured product ratios become similar. It should also be noted that the experimental C_2H_4:C_2H_5Cl ratios presented in Figure 4 show significant fluctuations which indicates that the product profiles shown in Figure 12 have possibly significant error margins as well.

At 577 K, both the predicted and measured acetaldehyde yields are much lower than those at 298 K, with the predictions slightly below the data. For clarity we did not include the yields of formaldehyde in the plot. Measured formaldehyde concentrations exceed at this temperature those of acetaldehyde by 7−8% percent at low conversion. Although the model captures this observation, the predicted difference is only about 5%. Finally, we compare the yields of CO and CO_2. As can be seen from the plot, the agreements are very good with the exception that the experimental data suggest a slight decline in CO_2 with ethane consumption whereas our model predicts a steady increase.

In addition to the comparisons shown for room temperature and 577 K we also performed calculations for Kaiser's measurements at 425 K. The quality of the predictions is similar to that at 577 K, although a rigorous quantitative comparison is not

possible, because Kaiser detected but did not quantify ethanol. Nevertheless, we found good agreement in the relative product yields. To conclude, we feel confident that our expanded mechanism is able to describe all important observations well. This enabled us to make extensive use of it to test for impact of secondary reactions on the primary products in the $C_2H_5 + O_2$ reaction.

Discussion

Our ultimate goal to obtain a good understanding of the low-temperature oxidation of ethane requires a reliable description of the $C_2H_5 + O_2$ reaction. In the preceding sections, we reported an approach to calculate apparent rate constants for this system, and these allowed us to satisfactorily reproduce a wide range of experimental data on the overall rate constant and direct products. For every case we investigated the impact of secondary reactions and showed that most of the data depend predominantly on the $C_2H_5 + O_2$ reaction. Because our kinetic analysis is based on a PES similar to those used by Sheng et al.[5] and Miller et al.,[6] one obvious question is what subtle differences are responsible for the improvements seen in this study. Specifically, we are interested in the significance of the following changes: (1) small variations in the PES, (2) the incorporation of tunneling, and (3) the increased stabilization rate. In addition, we will discuss the appropriateness of the kinetic analysis methods used, and finally we discuss implications of this study on future work.

Impact of PES Features. Results for the most significant stationary points on the PES from Miller et al., Sheng et al. and this work generally agree within 1 kcal/mol or better. This magnitude of error reflects the limits of many current ab initio studies. Some of the reasons for this limitation follow. (1) The commonly used ab initio methods are based on Hartree−Fock theory, which uses a single determinant wave function. Although the combination of subsequent steps at higher level of electron correlation and the extrapolation to an infinite basis set recovers most of the lost electron correlation, such an approach is still deficient. For example, it may miss spin−orbit coupling (at the CBS-QB3 level, a correction is only implicitly made for atoms) and contributions from other electronic states (multi-determinant contributions). (2) Contributions to the thermal energy are mainly calculated within the framework of the harmonic oscillator rigid rotor assumption. Although contributions from hindered rotors are treated separately in this study, coupling of these rotors to other internal or external rotors is only roughly accounted for (via the method chosen to calculate reduced moments of inertia). (3) We use bond additivity corrections to reduce systematic deviations between calculated and experimental enthalpies of formation. These corrections generally improve the absolute enthalpy values for stable species, but they may introduce new uncertainties with respect to relative enthalpy differences between reactants and transition states. The reason is that forming or breaking bonds in transition states cannot be corrected. This leaves us with an imbalance of bond corrections, which may lead to errors in the barrier height if the ignored bonds substantially contribute to errors of the electronic energy.

Given all these error sources the question arises how sensitive our predictions are to these uncertainties. In Figure 13, we present comparisons of the predicted temperature dependence of ethylene yields (relative to ethyl chloride) as a result of changing the barrier height for the concerted elimination by ±0.2 kcal/mol. All other parameters were kept constant. The results clearly demonstrate a high sensitivity of the ethylene yields to the size of this barrier. In this light the good accuracy of our

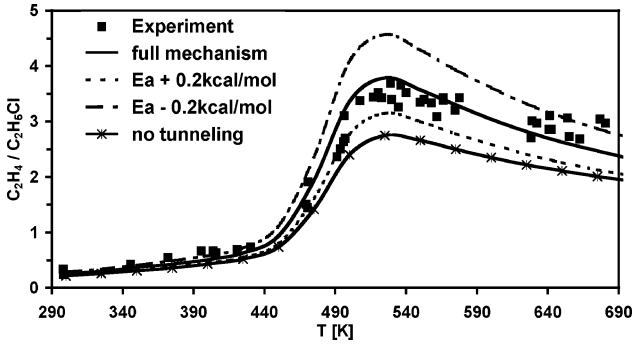

Figure 13. Impact of various modifications of the model on predicted temperature dependent ethylene yields (relative to ethylene chloride).

C_2H_4 and HO_2 predictions based on our CBS-QB3 PES must be regarded as fortuitous. In other words, it is not surprising that other researchers had to make small adjustments to improve their predictions. Although less extreme than for the concerted elimination, predictions of the $C_2H_4O + OH$ channel (as shown in Figure 7 and Figure 10) also depend on an accuracy of the barrier height for the isomerization of ethylperoxy to hydroperoxy ethyl, which can hardly be achieved with the CBS-QB3 method used here. The good agreement between predictions and experimental data must be seen, at least in part, as a fortunate cancellation of errors.

Impact of Tunneling Corrections. In Figure 13 we included predictions of the ethylene yields obtained with and without tunneling corrections for the high-pressure rate constants listed in Table 3. The incorporation of a tunneling correction clearly has an influence on the results, and this impact is largest around 500 K. At first glance, one might have expected that corrections for tunneling would be most important at the lowest temperatures, as is known to be the case for elementary reactions with activation barriers. But such an expectation does not take into account the fact that the recombination of C_2H_5 with O_2 proceeds on a surface without a barrier, and that the barrier for the concerted elimination is below the energy of the reactants. Because at low temperatures ethylene is produced via the "direct" chemically activated channel, the overall process does not experience any barrier and tunneling effects have little impact. With increasing temperature, contributions from the thermal dissociation of ethylperoxy become more important. Such contributions are small below 400 K, but by 500 K the "delayed" ethylene production starts to dominate. Because the thermal dissociation proceeds via a barrier, corrections for tunneling increase the overall rate constant and therefore the ethylene yield. At even higher temperatures, the impact of tunneling declines again as expected.

Wigner's analytic formula,[30] which was used in this study, is the simplest method to approximate tunneling effects because it requires at a given temperature only one input parameter, the imaginary frequency. Another frequently used method is based on the more realistic Eckart potential.[44] Schwartz et al.[45] demonstrated, on the basis of the reactions of OH radicals with CH_xF_{4-x}, that tunneling contributions calculated with Eckart potentials are very sensitive to PES features at and around the transition state. We performed preliminary calculations with a nonsymmetric Eckart function describing the barrier for the concerted elimination. These calculations resulted in correction factors that were only slightly higher than those obtained with Wigner's method. Although the differences were more severe for the isomerization reaction (e.g., at 600 K, $\kappa = 2.22$ and $\kappa = 2.62$ with Wigner's and Eckart's methods, respectively) they are still within 20% of each other. Therefore we believe that

the use of Wigner's correction formula is appropriate. Results obtained by Louis et al.[46] in their study of the reaction of OH radicals with CH_2Br_2 support this conclusion, as they found that TST predictions with Wigner's tunneling corrections actually agreed better with the experimental data than those done with Eckart potentials.

Impact of an Increased Stabilization Rate. An important outcome of this study is that the falloff at 298 K can only be predicted with an increased stabilization rate. This finding deserves additional discussion. As was explained in the results section, we were not able to reproduce the experimentally observed apparent C_2H_5 consumption rate constant at lower pressures when we used Lennard-Jones (LJ) parameters obtained from commonly used estimation methods. At this temperature the $C_2H_5 + O_2$ reaction is essentially a dual channel reaction: The first channel is the redissociation back to the reactants, and the second channel is the formation of stabilized $CH_3CH_2OO^\bullet$ radicals. (The $C_2H_4 + HO_2$ channel contributes, even at the lowest pressures, less than 3% to the consumption of chemically activated ethylperoxy and can be ignored in the context of this discussion.) Therefore the main cause for the discrepancies between the observed and predicted rates must be related to the stabilization process, or, more precisely, to the ratio of the collision stabilization and redissociation rates. This ratio depends basically on four factors: (1) the recombination rate constant, (2) the $CH_3CH_2OO^\bullet$ well depth, (3) the collision cross section, and (4) the energy transfer parameters.

The recombination rate constant was discussed earlier and appears to be rather well defined in terms of matching the higher pressure data. Changes in the well depth will affect the equilibrium constant, which in turn for a given recombination rate constant will affect the rate constant for redissociation. Such changes are only reasonable within a very restricted range, because the results from the ab initio calculations on one hand and the experimental observations on the other hand define its value accurately. Substantial changes of the well depth would have a profound impact on the predictions of product yields, in particular the temperature dependent yields of ethylene and HO_2. Our investigations showed that a variation of the well depth within these constraints could not reconcile the deviations between our predicted and the reported C_2H_5 consumption rates. This led us to consider adjusting the stabilization rate constant, either by increasing the number of collisions (meaning an increase of the collision cross section) or by making the collisions more efficient (increase the amount of energy transferred per collision).

The collision cross section is usually calculated on the basis of the Lennard-Jones (LJ) parameters σ_{LJ} and ϵ_{LJ} for both $CH_3CH_2OO^\bullet$ and the collider molecule. LJ cross sections have been used for many years, e.g., Fletcher et al.[47] A justification was given by Troe,[48] who showed that collision cross sections calculated from LJ parameters are very similar to kinetic cross sections deduced from trajectory calculations. But there are also a few cases known that indicate that the use of LJ cross sections is not always appropriate. Durant and Kaufman[49] for example demonstrated for the reactions of NO_2 that reactants with a permanent dipole moment seem to have a larger cross section than expected. A similar effect is believed to increase the collision efficiency of H_2O in the reaction of $H + O_2$.[50] $CH_3CH_2OO^\bullet$ also has a permanent dipole moment, calculated to be ~3 D, and if we compare our estimated LJ collision cross section with that obtained with Durant and Kaufman's estimation method, we find that the second method yields a ~25% larger cross section. This increase, however, is not large enough to explain the observed differences with the experiments.

The energy transfer probability within the framework of the modified strong collision (MSC) assumption is given by the collision efficiency factor β_c (which, in turn, is related to $\langle\Delta E_{all}\rangle$). We calculated this parameter in this study with the improved procedure given by Gilbert et al.[51] Essentially the β_c value is defined in such a way that the MSC method reproduces results of detailed master equation analysis as closely as possible. In the results section we verified this for the predictions of the total rate constant and for the temperature dependence of HO_2 yields. The results obtained with the ME and MSC methods showed no indication that the β_c values used in this study leads to unreasonable predictions. In addition to our own steady-state codes, we employed MultiWell,[40] a program that solves the master equation stochastically. In these calculations we used the exponential down model for energy transfer together with a $\langle\Delta E_{down}\rangle$ value of 200 cm^{-1}; the same value was used by DeSain et al.[9] in their calculations. The MultiWell results also underestimated the overall rate coefficient; hence the deviations must be due to a more fundamental problem than an unfortunate choice of β_c. Nevertheless, one might ask the question what value of $\langle\Delta E_{all}\rangle$ would be needed to obtain the desired increase in stabilization. We found that a $\langle\Delta E_{all}\rangle$ value of approximately -350 cm^{-1} (4 times higher than our initial value) for He leads to a good match to the experimental data. However, this value appears to be unusually high. For example, we found that $\langle\Delta E_{all}\rangle = -96$ cm^{-1} successfully predicted the thermal dissociation data for ethoxy as measured by Caralp et al.[52] Therefore we decided to keep the energy transfer parameters at their regular values and multiply the stabilization rate by a correction factor of 2.4. This value was used in all our calculations and for all colliders. We emphasize that we cannot distinguish whether an increase in collision cross section or an increase in the energy transferred per collision is a more appropriate approach to increase the collisional deactivation rate to the value that is needed to fit the falloff data.

The unusually high stabilization efficiency demands at least an attempt of an explanation. A possible cause could be that the first excited electronic state of ethylperoxy is involved in the energy transfer process. The importance of this $^2A'$ state was already discussed by Pilling et al.,[53] Reinstra-Kiracofe et al.[3], and Andersen et al.,[54] although these authors focused on a possible role of the $^2A'$ state in the concerted elimination reaction. On the basis of a few trajectory calculations, Andersen et al. conclude that vibronic couplings between the two low-lying electronic states exist close to the transition state of the concerted elimination but also in the vicinity of the $C_2H_5 + O_2$ entrance channel. These couplings could provide an effective mechanism to convert the $^2A''$ ground state to the $^2A'$ electronically excited state. Ethylperoxy in its $^2A'$ state may remain trapped in it, because this state only correlates with the endothermic $C_2H_5 + {}^1O_2$ channel. The effective stabilization rate would be higher. Stark[55] uses similar arguments to explain the high yields of epoxides in the addition of peroxy radicals to alkenes.

Transitions from one electronic state to another are well-known in the literature (e.g., for CH_2 [56]). If these transitions require collisions to induce the necessary coupling of the involved states, one can find a strong collider mass dependence on the transition rate. This might explain why O_2 appears to be a stronger collider compared to He than usual as we saw in the pressure dependent C_2H_4 yield studies. Nevertheless, the suspicion that the second electronic state is involved is just a

hypothesis and a more detailed characterization of both electronic states, including possible couplings between them, is needed to verify this idea.

Another potential explanation is that the density of states close to threshold is not described properly with our QRRK model. It has been shown by Barker et al.[57] that changes in transition state models, which affect the state density, can dramatically affect the value of the energy transfer step size required. However, the fact that our models, based on estimating the density of states based on heat capacities, gave very similar results to Multiwell, which uses a direct count method, suggests that our estimate is consistent with the direct count method. A similar conclusion was reached previously.[58] At this stage we only note that with the adjustment of the stabilization rate, we observed good agreement with most experiments, not only for the overall rate constants but also for individual product channels at different temperatures and pressures.

Effect of the Analysis Methods on *k*(*T*,*P*). Most of the calculations described in this study were done with a steady state QRRK/MSC code. The choice to describe the stabilization process with the modified strong collision (MSC) method leads to a bimodal distribution function of each isomer involved in the reaction. The isomer is either excited or stabilized. The stabilized species are thermalized products of the chemically activated reaction, which are formed, possibly after a series of isomerization steps, via deactivating collisions with the bath gas. The excited states of the isomers are treated as transient species, and they will exist after a short initial period in a steady state concentration. The steady state concentration depends on the rates of formation and consumption and can easily be determined from the $k(E)$ information. We use QRRK theory to calculate $k(E)$ and $\rho(E)$ for all species and reaction channels. The results of the analysis described above are apparent rate constants for the reaction of the reactants to the stable isomers or to the bimolecular products. We conceptually separate these reactions from subsequent thermal dissociation reactions of the isomers. By doing so we generate reactions on two different time scales: (1) Chemically activated processes proceed on a fast time scale because they include collisional deactivation channels, which proceed on the order of the collision frequency. We refer to these reactions as "prompt" or "direct" channels. (2) Unimolecular reactions of stabilized adducts occur on a longer time scale. We call products from these reactions "delayed".

Despite its successes,[59,60] the use of QRRK/MSC theory to analyze chemically activated reactions has been criticized in the past. Therefore it is appropriate to address its weaknesses and the validity of the assumptions made. This will be done in the following few paragraphs by focusing on individual aspects of the method: (a) the QRRK theory, (b) the MSC assumption, and (c) the steady-state approach.

The calculation of $k(E)$ is central to any analysis method of pressure dependent reactions. The most accurate method to calculate this function within a statistical framework is the RRKM theory. However, RRKM calculations rely on accurate detailed molecular information for all reactants and transition states. At low temperatures, the results depend largely on the accuracy of individual low-frequency modes and internal rotations. Because calculated frequencies of large amplitude vibrations often have significant errors, they can easily jeopardize the reliability of RRKM calculations. QRRK calculations are in principle less accurate than RRKM calculations, but they have the advantage that they require only representative frequencies as input; these are readily obtained from heat capacities. Therefore QRRK results depend far less on the accuracy of individual low-frequency modes than RRKM results. Although we do not want to argue that QRRK theory is the more appropriate choice for this study, we feel that its use will not necessarily introduce flaws in the final kinetic analysis presented here. As discussed previously, the calculated $k(E)$ and $\rho(E)$ in this study yielded room-temperature falloff curves that are quite similar to those predicted using the stochastic method[40] based on a inverse Laplace transform to calculate $k(E)$ and direct counting to compute $\rho(E)$.

A more severe approximation is the use of the MSC approach to describe energy transfer. This approach leads to the bimodal distribution mentioned above. In the case of the $C_2H_5 + O_2$ reaction, excited ethylperoxy is distributed at an energy above the reactants and stabilized ethylperoxy is deep in the well. A more realistic view of the stabilization process would envision that weak collisions first deactivate these excited ethylperoxy radicals below the entrance energy, and consecutive collisions later lead to thermalized ethylperoxy. Because the barrier for the concerted elimination is below the energy of the reactants, this channel would still be open after the first few collisions. Thus it appears that the MSC and the ME approach should yield clearly different product distributions. One would expect that the ME treatment yields higher prompt ethylene and HO_2 yield than the MSC analysis. Our HO_2 results at low temperatures (Figure 9) support this analysis, but they also show that the differences between both models are surprisingly small. One reason for such a small difference may be that the concerted elimination barrier is only "a few collisions" below the entrance channel, so that the lifetime of chemically activated ethylperoxy with an energy below the entrance channel but above this barrier may be too short to significantly alter the product yields in the ME analysis. In other words, the MSC approximation appears to be a reasonable model for this reaction system. Because the energy transfer parameters ($\langle\Delta E_{all}\rangle$ or $\langle E_{down}\rangle$, respectively) used in these calculations are estimated values, with little direct connection to experiment, we believe that the uncertainties in these values have a larger impact on the results than the choice of the energy transfer model itself. Going back to the room-temperature HO_2 yields (Figure 9), it is important to note that the differences between the calculated and measured values are far too large to be explained by the choice of the energy transfer model.

The ability to describe complex reaction systems in terms of time independent rate coefficients is a crucial requirement to build conventional reaction mechanisms. Time independent rate coefficients can only be obtained if energy relaxation is fast compared to the chemical processes, so that the later can be separated in time from energy transfer. This can easily be seen from

$$k(T,t) = \int_{E_0}^{\infty} k(E)\, g(E,t)\, \mathrm{d}E$$

Here $k(E)$ represent an effective energy dependent rate constant, and $g(E,t)$ is the time dependent distribution function. Because only $g(E,t)$ is a function of time, we immediately notice that a constant distribution function ($g(E)$) directly leads to a time independent rate constant. Any attempt to describe the $C_2H_5 + O_2$ reaction with time independent apparent rate constants therefore automatically assumes that the distribution is in steady state. The major question is how fast the steady-state condition can be achieved, or, in other words, how much of the chemistry happens prior to reaching the steady-state condition.

Miller et al. investigated the reaction of $C_2H_5 + O_2$ by solving the time dependent master equation. They converted the

solutions to time independent rate constants and found that predictions with both sets agree well with each other (cf. ref 9, Figure 4). A second indication that time independent rate constants provide an adequate description of the reaction can be seen from our results. We are able to predict the "prompt" and "delayed" ethylene yields reasonably well over a wide range of temperatures and pressures. We are also able to accurately predict the time profile of HO_2 at 624 K. These varying conditions lead to changes in the stabilization and reaction rates by many orders of magnitude, but we did not see any indication for a breakdown of the steady-state assumption in any case.

Implications for Future Work. The starting point for this work was the assumption that the wealth of experimental data of the $C_2H_5 + O_2$ reaction provides a stringent test set that will allow us to thoroughly validate our kinetic analysis of this system. Although this assumption proved to be largely fulfilled, we realized the impact of secondary reactions on many of these data sets, even those that involved stable products such as ethylene or ethylene oxide. The extended mechanism that we used to account for secondary chemistry performed well for all species but OH. Our failure to predict the longer time OH profiles measured by DeSain et al. is disturbing. Although we have reason to believe that the measurements of the peak OH concentrations confirm our kinetic description of the OH producing channels in the $C_2H_5 + O_2$ reaction, the inability to predict the longer time behavior of OH implies that our extended mechanism is not satisfactory, at least as far as reactions of OH are concerned. One reaction type that warrants additional attention is that between alkyl radicals and HO_2. Not only do these reactions play a significant role in the experiments of DeSain et al., but also they have a broader importance in the low-temperature oxidation chemistry because they effectively convert less reactive HO_2 radicals into reactive OH radicals. At the same time the alkyl species is converted to an alkoxy radicals, which in its reaction with excess oxygen, regenerates HO_2 and a reactive aldehyde. Although some limited information about these reactions exist,[61,62] additional experimental and theoretical efforts are necessary. It would also be worthwhile to investigate the impact of the precursor molecule and photodissociation fragment on the OH profiles. In this context new experimental profiles obtained with a different source for C_2H_5 would be very helpful.

A second implication of this study is related to the general model for the low-temperature oxidation of alkanes. This model contains two sources for chain branching. The first source starts with the reaction of hydroperoxyalkyl radicals with O_2. This chemically activated reaction has several important product channels, which all subsequently produce two or more reactive species (e.g., OH radicals). The second source of chain branching begins with a hydrogen atom abstraction by alkylperoxy radicals to form an alkylhydroperoxide plus a new radical. Alkylhydroperoxides start to decompose at temperatures of the NTC region (600−800 K) to form OH and alkoxy radicals. In the case of ethane ignition, the isomerization step, which is the prerequisite step of the first chain branching sequence, has a significantly higher barrier than the barrier for concerted elimination. But even if isomerization occurs, at lower pressures most of the initially formed excited hydroperoxyethyl radicals will directly dissociate to the products $C_2H_4O + OH$ and $C_2H_4 + HO_2$ and only small concentrations of stabilized hydroperoxyethyl are available for the second oxygen addition step. Our results thus suggest that the formation and subsequent dissociation of ethylhydroperoxide is the only effective source for chain branching. We are in the process of updating our rate expressions for $CH_3CH_2OO^\bullet$ abstraction reactions[63] to provide improved estimates of the production rate of ethylhydroperoxide. With these updates in place, we plan to address the issue of low-temperature ethane oxidation. The good agreement of our mechanistic predictions to the various data on different aspects of the $C_2H_5 + O_2$ system makes us confident that this submechanism is now well established.

Conclusion

We have calculated the PES for the $C_2H_5 + O_2$ system at the CBS-QB3 level. Further improvements are achieved by incorporating bond additivity corrections to the energies. Tunneling was included in high-pressure rate constants using Wigner's formula. The reaction was analyzed using steady state QRRK/MSC as well as QRRK/ME methods. Results from both methods are comparable. The collision cross section was increased to better predict the falloff data. The resulting pressure dependent reaction mechanism accurately predicts a wide range of experimental results on overall rate constants and direct products such as ethylene, ethylene oxide, HO_2, and possibly OH. By using an extended mechanism, we showed that secondary reactions have an impact on the products in the $C_2H_5 + O_2$ reaction. However, in most cases these corrections were small.

Our kinetic analysis of the $C_2H_5 + O_2$ system confirmed our suspicion that the concerted elimination reaction effectively shuts down chain branching via the "second oxygen addition mechanism". Consequently, to maintain sufficient reactivity of ethane/oxygen systems at low temperature, new chain branching reactions need to be identified. One possibility that warrants further consideration is hydrogen abstraction by RO_2 radicals (rxn-2) as one additional source of chain branching. Finally, we feel that the success in predicting so many aspects of the $C_2H_5 + O_2$ system accurately makes this subset suitable to be incorporated into a model of ethane oxidation at low temperatures.

Acknowledgment. We acknowledge Prof. J. W. Bozzelli, Dr. C. Sheng, Dr. E. W. Kaiser, and Dr. C. A. Taatjes for helpful discussions. Early stages of this research were partially supported by a grant from ExxonMobil Research and Engineering Company.

Supporting Information Available: We provide the expanded mechanism for 1 atm O_2 (collider) in Arrhenius form together with the thermodynamic properties for all the species used in the mechanism in NASA polynomial format. Pressure dependent apparent rate constants for the $C_2H_5 + O_2$ system valid for 0.0001−100 atm and 300−850 K with O_2 and He as colliders are also included in Chebyshev format. This material is available free of charge via the Internet at http://pubs.acs.org.

References and Notes

(1) Walker, R. W.; Morley, C. Basic Chemistry of Combustion. In *Low-Temperature Combustion and Autoignition*; Pilling, M. J., Ed.; Elsevier: Amsterdam, 1997; Vol. 35, p 1.

(2) Ignatyev, I. S.; Xie, Y.; Allen, W. D.; Schaefer, H. F., III. *J. Chem. Phys.* **1997**, *107*, 141.

(3) Rienstra-Kiracofe, J. C.; Allen, W. D.; Schaefer, H. F., III. *J. Phys. Chem. A* **2000**, *104*, 9823.

(4) Baldwin, R. R.; Dean, C. E.; Walker, R. W. *J. Chem. Soc., Faraday Trans. 2* **1986**, *82*, 1445.

(5) Sheng, C. Y.; Bozzelli, J. W.; Dean, A. M.; Chang, A. Y. *J. Phys. Chem. A* **2002**, *106*, 7276.

(6) Miller, J. A.; Klippenstein, S. J.; Robertson, S. H. *Proc. Combust. Inst.* **2000**, *28*, 1479.

(7) Miller, J. A.; Klippenstein, S. J. *Int. J. Chem. Kinet.* **2001**, *33*, 654.

(8) Miller, J. A. *Faraday Discuss.* **2001**, *119*, 461.
(9) Desain, J. D.; Klippenstein, S. J.; Miller, J. A.; Taatjes, C. A. *J. Phys. Chem. A* **2003**, *107*, 4415.
(10) Slagle, I. R.; Feng, Q.; Gutman, D. *J. Phys. Chem.* **1984**, *88*, 3648.
(11) Plumb, I. C.; Ryan, K. R. *Int. J. Chem. Kinet.* **1981**, *13*, 1011.
(12) Kaiser, E. W.; Wallington, T. J.; Andino, J. M. *Chem. Phys. Lett.* **1990**, *168*, 309.
(13) McAdam, K. G.; Walker, R. W. *J. Chem. Soc., Faraday Trans. 2* **1987**, *83*, 1509.
(14) Wallington, T. J.; Andino, J. M.; Kaiser, E. W.; Japar, S. M. *Int. J. Chem. Kinet.* **1989**, *21*, 1113.
(15) Wagner, A. F.; Slagle, I. R.; Sarzynski, D.; Gutman, D. *J. Phys. Chem.* **1990**, *94*, 1853.
(16) Kaiser, E. W.; Rimai, L.; Wallington, T. J. *J. Phys. Chem.* **1989**, *93*, 4094.
(17) Kaiser, E. W.; Lorkovic, I. M.; Wallington, T. J. *J. Phys. Chem.* **1990**, *94*, 3352.
(18) Kaiser, E. W. *J. Phys. Chem.* **1995**, *99*, 707.
(19) Baldwin, R. R.; Pickering, I. A.; Walker, R. W. *J. Chem. Soc., Faraday Trans. 1* **1980**, *76*, 2374.
(20) Kaiser, E. W. *J. Phys. Chem. A* **2002**, *106*, 1256.
(21) Clifford, E. P.; Farrell, J. T.; Desain, J. D.; Taatjes, C. A. *J. Phys. Chem. A* **2000**, *104*, 11549.
(22) Montgomery, J. A., Jr.; Frisch, M. J.; Ochterski, J. W.; Petersson, G. A. *J. Chem. Phys.* **1999**, *110*, 2822.
(23) Frisch, M. J.; Trucks, G. W.; Schlegel, H. B.; Scuseria, G. E.; Robb, M. A.; Cheeseman, J. R.; Zakrzewski, V. G.; Montgomery, J. A., Jr.; Stratmann, R. E.; Burant, J. C.; Dapprich, S.; Millam, J. M.; Daniels, A. D.; Kudin, K. N.; Strain, M. C.; Farkas, O.; Tomasi, J.; Barone, V.; Cossi, M.; Cammi, R.; Mennucci, B.; Pomelli, C.; Adamo, C.; Clifford, S.; Ochterski, J.; Petersson, G. A.; Ayala, P. Y.; Cui, Q.; Morokuma, K.; Malick, D. K.; Rabuck, A. D.; Raghavachari, K.; Foresman, J. B.; Cioslowski, J.; Ortiz, J. V.; Baboul, A. G.; Stefanov, B. B.; Liu, G.; Liashenko, A.; Piskorz, P.; Komaromi, I.; Gomperts, R.; Martin, R. L.; Fox, D. J.; Keith, T.; Al-Laham, M. A.; Peng, C. Y.; Nanayakkara, A.; Challacombe, M.; Gill, P. M. W.; Johnson, B.; Chen, W.; Wong, M. W.; Andres, J. L.; Gonzalez, C.; Head-Gordon, M.; Replogle, E. S.; Pople, J. A. *Gaussian 98*, Revision A.11; Gaussian, Inc.: Pittsburgh, PA, 1998.
(24) Schaftenaar, G.; Noordik, J. H. *J. Comput.-Aided Mol. Design* **2000**, *14*, 123.
(25) East, A. L. L.; Radom, L. *J. Chem. Phys.* **1997**, *106*, 6655.
(26) Kilpatrick, J. E.; Pitzer, K. S. *J. Chem. Phys.* **1949**, *17*, 1064.
(27) Wood, G. P. F.; Henry, D. J.; Radom, L. *J. Phys. Chem. A* **2003**, *107*, 7985.
(28) Coote, M. L. *J. Phys. Chem. A* **2004**, *108*, 3865.
(29) Petersson, G. A.; Malick, D. K.; Wilson, W. G.; Ochterski, J. W.; Montgomery, J. A., Jr.; Frisch, M. J. *J. Chem. Phys.* **1998**, *109*, 10570.
(30) Wigner, E. *Z. Phys. Chem.* **1932**, *B19*, 203.
(31) Chang, A. Y.; Bozzelli, J. W.; Dean, A. M. *Z. Phys. Chem.* **2000**, *214*, 1533.
(32) Bozzelli, J. W.; Chang, A. Y.; Dean, A. M. *Int. J. Chem. Kinet.* **1997**, *29*, 161.
(33) Venkatesh, P. K.; Chang, A. Y.; Dean, A. M.; Cohen, M. H.; Carr, R. W. *AIChE J.* **1997**, *43*, 1331.
(34) Naik, C.; Carstensen, H.-H.; Dean, A. M. Reaction Rate Representation Using Chebyshev Polynomials. Presented at the Western States Section 2002 Spring Meeting of the Combustion Institute, San Diego, CA, 2002.
(35) Kee, R. J.; Rupley, F. M.; Miller, J. A.; Coltrin, M. E.; Grcar, J. F.; Meeks, E.; Moffat, H. K.; Lutz, A. E.; Dixon-Lewis, G.; Smooke, M. D.; Warnatz, J.; Evans, G. H.; Larson, R. S.; Mitchell, R. E.; Petzold, L. R.; Reynolds, W. C.; Caracotsios, M.; Steward, W. E.; Glarborg, P.; Wang, C.; Adigun, O. *Chemkin Collection*, Release 3.6; Reaction Design, Inc.: San Diego, CA, 2000.
(36) Knyazev, V. D.; Slagle, I. R. *J. Phys. Chem. A* **1998**, *102*, 1770.
(37) Blanksby, S. J.; Ramond, T. M.; Davico, G. E.; Nimlos, M. R.; Kato, S.; Bierbaum, V. M.; Lineberger, W. C.; Ellison, G. B.; Okumura, M. *J. Am. Chem. Soc.* **2001**, *123*, 9585.
(38) Dobis, O.; Benson, S. W. *J. Phys. Chem. A* **1997**, *101*, 6030.
(39) Timonen, R. S.; Gutman, D. *J. Phys. Chem.* **1986**, *90*, 2987.
(40) Barker, J. R. *Int. J. Chem. Kinet.* **2001**, *33*, 232.
(41) Desain, J. D.; Klippenstein, S. J.; Miller, J. A.; Taatjes, C. A. *J. Phys. Chem. A* **2004**, *108*, 7127.
(42) Niki, H.; Maker, P. D.; Savage, C. M.; Breitenbach, L. P. *J. Phys. Chem.* **1982**, *86*, 3825.
(43) Wallington, T. J.; Gierczak, C. A.; Ball, J. C.; Japar, S. M. *Int. J. Chem. Kinet.* **1989**, *21*, 1077.
(44) Eckart, C. *Phys. Rev.* **1930**, *35*, 1303.
(45) Schwartz, M.; Marshall, P.; Berry, R. J.; Ehlers, C. J.; Petersson, G. A. *J. Phys. Chem. A* **1998**, *102*, 10074.
(46) Louis, F.; Gonzalez, C.; Huie, R. E.; Kurylo, M. J. *J. Phys. Chem. A* **2000**, *104*, 2931.
(47) Fletcher, F. J.; Rabinovitch, B. S.; Watkins, K. W.; Locker, D. J. *J. Phys. Chem.* **1966**, *70*, 2823.
(48) Troe, J. *J. Phys. Chem.* **1979**, *83*, 114.
(49) Durant, J. L.; Kaufman, F. *Chem. Phys. Lett.* **1987**, *142*, 246.
(50) Michael, J. V.; Su, M.-C.; Sutherland, J. W.; Carroll, J. J.; Wagner, A. F. *J. Phys. Chem. A* **2002**, *106*, 5297.
(51) Gilbert, R. G.; Luther, K.; Troe, J. *Ber. Bunsen-Ges. Phys. Chem.* **1983**, *87*, 169.
(52) Caralp, F.; Devolder, P.; Fittschen, C.; Gomez, N.; Hippler, H.; Mereau, R.; Rayez, M. T.; Striebel, F.; Viskolcz, B. *Phys. Chem. Chem. Phys.* **1999**, *1*, 2935.
(53) Pilling, M. J.; Robertson, S. H.; Seakins, P. W. *J. Chem. Soc., Faraday Trans.* **1995**, *91*, 4179.
(54) Andersen, A.; Carter, E. A. *J. Phys. Chem. A* **2002**, *106*, 9672.
(55) Stark, M. S. *J. Am. Chem. Soc.* **2000**, *122*, 4162.
(56) Bley, U.; Temps, F. *J. Chem. Phys.* **1993**, *98*, 1058.
(57) Barker, J. R.; Lohr, L. L.; Shroll, R. M.; Reading, S. *J. Phys. Chem. A* **2003**, *107*, 7434.
(58) Bozzelli, J. W.; Chang, A. Y.; Dean, A. M. *Int. J. Chem. Kinet.* **1997**, *29*, 161.
(59) Bozzelli, J. W.; Dean, A. M. *J. Phys. Chem.* **1993**, *97*, 4427.
(60) Dean, A. M.; Bozzelli, J. W. Combustion Chemistry of Nitrogen. In *Gas-phase Combustion Chemistry*; Gardiner, W. C., Ed.; Springer: New York, 2000; p 125.
(61) Tsang, W.; Hampson, R. F. *J. Phys. Chem. Ref. Data* **1986**, *15*, 1087.
(62) Bozzelli, J. W.; Dean, A. M. *J. Phys. Chem.* **1990**, *94*, 3313.
(63) Carstensen, H.-H.; Dean, A. M. *Proc. Combust. Inst.* **2004**, *30*, 995.